

AD-A160 362

METRIC CALIBRATION OF THE MILLSTONE HILL L-BAND RADAR

1/1

(U) MASSACHUSETTS INST OF TECH LEXINGTON LINCOLN LAB

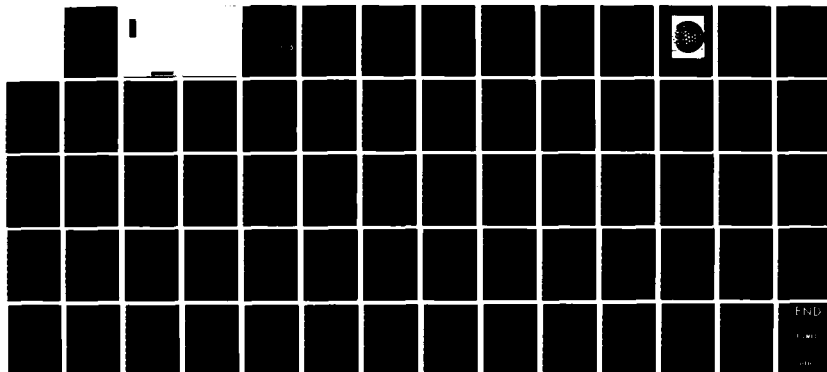
E M GAPOSCHKIN 19 AUG 85 TR-721 ESD-TR-85-173

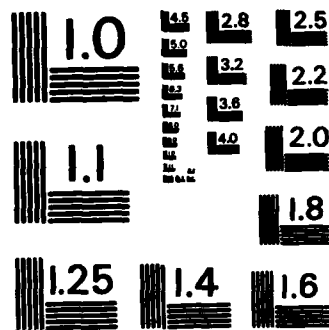
UNCLASSIFIED

F19628-85-C-0002

F/G 17/9

NL





MICROCOPY RESOLUTION TEST CHART
NATIONAL BUREAU OF STANDARDS-1963-A

**MASSACHUSETTS INSTITUTE OF TECHNOLOGY
LINCOLN LABORATORY**

**METRIC CALIBRATION
OF THE MILLSTONE HILL L-BAND RADAR**

E.M. GAPOSCHKIN

Group 91

TECHNICAL REPORT 721

19 AUGUST 1985

**DTIC
ELECTE
OCT 17 1985
S D
B**

Approved for public release; distribution unlimited.

LEXINGTON

MASSACHUSETTS

Abstract

The precision Lageos orbit is used for near real time calibration of the Millstone Hill Radar 1MHz chirped frequency domain tracker. With independent tracking data, the range calibration is given to $\approx 1m$, with Millstone data the range calibration is given to $\approx 5m$. The range rate is an unbiased measurement, with an accuracy of $\approx 1mm/sec$. The azimuth and elevation are calibrated to $0^\circ.020$ and $0^\circ.002$ respectively. Tables of calibration constants are given.



Accession For		
NTIS GRAM	<input checked="" type="checkbox"/>	
DTIC TAB	<input type="checkbox"/>	
Unannounced	<input type="checkbox"/>	
Justification		
By _____		
Distribution/		
Availability Codes		
Avail and/or		
Dist	Special	
A-1		

Contents

Abstract	iii
1. Introduction	1
2. Objectives	2
3. Method	4
4. Calibration Model	9
5. Refraction	28
6. Orbital Results	38
7. Prediction Accuracy	47
8. Summary & Conclusions	50
9. Acknowledgements	52
References	53
Appendix A - Calibration Constants	55

1. Introduction

Calibration of metric data from the Millstone Hill Radar requires an external standard. The basic observables (time delay, delay rate, etc) must be converted into metric quantities using a calibration model. The parameterization of the calibration model (i.e. the transformation from observables to metric quantities) comes from the system designer. The numerical values used in the calibration model come from the calibration against an external standard. We review here the calibration model, data reduction methods used at the Millstone Hill Radar, and the methods used to obtain the calibration coefficients. Quantities that are measured within the system, and used to determine the observable, such as peak power, bandwidth, and droop, are not considered part of calibration. The external standard is a satellite (Lageos, 1976 039 01, SDC#8820) with a very well known orbit. Therefore the methods used in this analysis can be applied to other sensors. The limitations of this approach will also be described. Because the metric accuracy of the radar is continually being improved, so too are the calibration techniques. However, we expect this method to provide the most accurate independent calibration of a metric radar. We describe here the present status and results from this calibration effort, in preparation for the next overall improvement in system performance.

2. Objectives

The Millstone Hill Radar is used primarily for space surveillance of objects in orbit around the earth. The radar operates at a fundamental frequency of 1295 MHz, and can observe targets from close earth orbit (several hundred kilometers range) to geosynchronous orbit (6 earth radii or 42000 Km) and beyond, depending, of course, on radar cross section. Recent modernization and refined signal processing methods (1) give an expected precision of better than 1m in range and 1mm/sec in range rate, for Lageos. The present mechanical azimuth and elevation encoders can provide an angle precision of $0^{\circ}.002$. The task of calibration then, is to transform this precision into accuracy.

In addition to the need for high accuracy, there is timeliness. Data taken with the radar is generally used within minutes. Therefore, the calibration would best be available immediately. Of course, refined calibration constants are always useful in a posteriori analysis.

The reduction of basic observables (e.g. time delay) to metric quantities (e.g. range) also requires that certain environmental corrections be made. The most important is tropospheric and ionospheric refraction. This study describes the simple models used. It is quite likely that limitations in calculating refraction imposes the ultimate limit on absolute accuracy.

In summary we intend to provide near real time calibration of the Millstone Hill Radar to one meter and one millimeter per second, or better.

In addition to providing absolute calibrated metric data, in near real time, the calibration procedure also provides the following capabilities:

- 1) Monitor of system performance.
- 2) Identify and flag error conditions, e.g. clock malfunction.
- 3) Monitor and assess environmental parameters.
- 4) Provide rapid assessment of system modification, enhancements, etc.

3. Method

Our independent yardstick for calibration is the Lageos satellite. The orbit of Lageos (Fig. 1) is the best known orbit in the solar system, that is to say it can be known in a geocentric inertial reference frame with an accuracy of better than 20cm. The orbital and physical characteristics of Lageos are given in Table I.

TABLE I

LAGEOS CHARACTERISTICS

Semi-major axis	12000km
eccentricity	0.006
inclination	109°.0
Mean Motion	6.6 rev/day
Shape	sphere
Mass	407.00 kg
radius	30.0 cm
surface	aluminum
core	brass-copper
reflectivity coeff.	1.002
laser ranging	426 cube corner reflectors
radar cross section (L-Band)	0.28 m ²

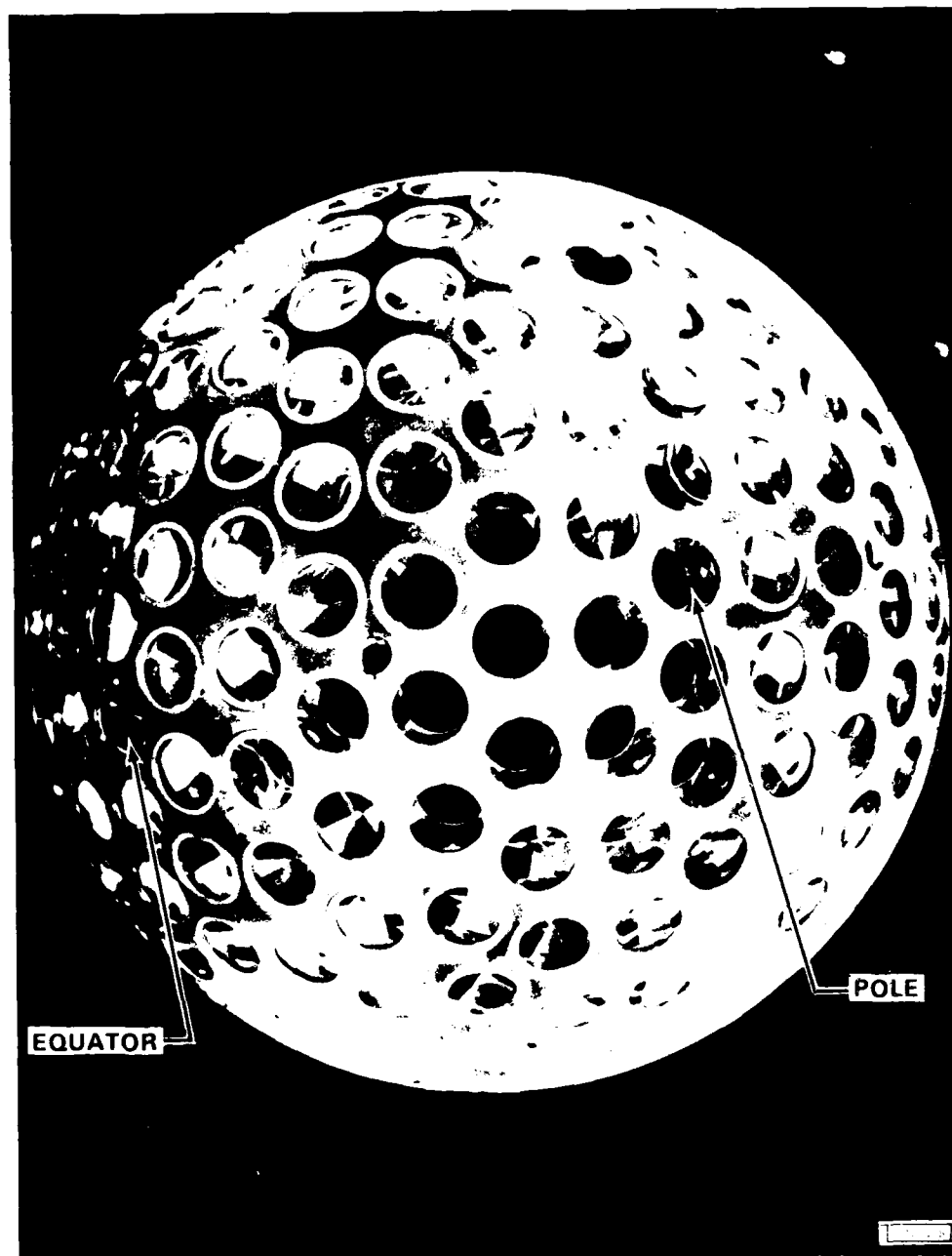


Fig. 1. The Lageos satellite.

These characteristics make Lageos an excellent calibration target for a number of reasons:

- 1) The altitude and eccentricity reduce the effects of the anomalous geopotential. The small area to mass ratio reduces the effects of non-gravitational forces. The spherical shape makes these forces easier to compute. From an orbital accuracy standpoint, it is optimized.
- 2) Lageos has a good radar cross section at L-Band, and precision metric observations are possible.
- 3) Lageos has good station geometry, which allows determination of azimuth and elevation dependent calibration parameters.
- 4) The laser cube corners allow observations with laser ranging systems. There is a global network of laser tracking systems with tracking accuracy of better than 10cm. These observations allow determination of the Lageos orbit to comparable accuracy.

While the laser ranging systems have the capability to provide data with an accuracy of better than 10 cm, it requires a number of post processing corrections to achieve this accuracy. Laser ranging data is available within minutes of the observation without these refinements, and is known as quick look data. The accuracy of quick look laser data ranges from 10 cm to 50 cm. It is the quick look data that we exploit in the real time calibration system.

There are four modes of using Lageos for calibration:

1) Based on the metric data alone, an orbit is determined with calibration parameters, i.e. simultaneous recovery of the state vector at some epoch, and the sought calibration parameters. This is rather time consuming (slow) in that it will use data from many passes over several days to get the benefit of orbital constraints, and a complete force model is needed to achieve submeter accuracy. Therefore it is not suitable for near real time application.

2) With a state vector derived, say as in 1) above, the orbit can be predicted to the time of observation. This prediction can be compared with the actual observation, and the difference can be used to obtain calibration parameters. This method is limited by the degradation of orbital accuracy as the observation time gets far from the epoch or data interval used to obtain the state vector. However it is fast.

3) Based on independent tracking data, say laser ranging, a precision orbit is determined. Then, the differences between that reference orbit, and the observation can be used to obtain calibration values. This approach involves heavy computation as in 1) above. It has the advantage of a more accurate orbit, and independent determination of orbit and calibration parameters. This is the most accurate method.

4) With a state vector derived in 3) above, one can proceed as in 2). This has the same relative advantages and drawbacks. The orbital accuracy is better, and the extrapolation accuracy will also be better.

The basic results reported here are derived from 1, 2, and 3 above. Mode 2 (and Mode 4) have been implemented in a software package described by Kantrowitz (2) and Byers (3) and a few remarks about it are in order. The precision orbit computation is described in section 6 below. The program (DYNAMO) has an output option to generate predicted observations (azimuth, elevation, range, range rate) from an initial state vector. The predictions are made for every pass, typically for one week to 10 days after the last observation used in the orbit fit. These predictions are made for arbitrary times, and the calibration software uses numerical interpolation to compute the observed quantities at the time of observation. The interpolation methods and accuracy assessment is given by Kantrowitz (2). It has been found acceptable to use a time spacing of 1 minute for the predicted data points.

4. Calibration Model

There are three modes of tracking with the Millstone Hill Radar:

- 1) Coded pulse, used primarily for acquisition.
- 2) Chirped pulse, with up to 1MHz bandwidth, with the frequency domain tracker. This tracker uses coherent integration to improve signal to noise ratio, and a fast fourier transform (FFT) to estimate the doppler shift for estimation of line of sight velocity. The chirped receive pulse is deramped in analog and sampled with the matched pulse being reconstructed in either a hardwired correlator or in an Array Processor. In current operation the two methods should generate the same result. However we observe the correlator and AP to have different range calibration constants.
- 3) Chirped pulse, with up to 1MHz bandwidth, with the time domain tracker. This tracker, designed by Raup (1) provides metric data on non-coherent targets with an accuracy approaching that which the frequency domain tracker achieves on coherent targets. When fully implemented one can expect that, by invoking coherency assumptions where appropriate, significantly improved range rate estimates will be possible. Since the time domain and frequency domain trackers are processing the same information they should give the same results. That means any difference must be software induced. Since they should both be

unbiased estimates of the same quantity, the result should be the same to within the formal uncertainty. This does not seem to be the case.

Each tracking mode should have its own mode dependent calibration model. In fact, only for the frequency domain data (2) is sufficient tracking data in hand to quantify the calibration constants. Preliminary data is available for the time domain tracker, and the coded pulse and correlator data remain to be investigated. In all cases a basic general calibration model is adopted with some mode dependent parameters. Therefore, the main results available are for the chirped, 1MHz, frequency domain tracker. Preliminary results on the other trackers (modes of operation) will be given when available. The basic calibration model is described in Table II.

TABLE II

CALIBRATION MODEL

Observable	Calibration Parameter	Depends On
Range	Bias	
Range Rate	Bias=0	
Elevation	Bias Droop	elevation
Azimuth	Bias Traverse Misalignment	elevation elevation, azimuth
Refraction	Tilt	level sensors elevation, elevation rate, ionosond, refractometer

Using the frequency domain tracker we have found that range rate data is unbiased with an accuracy of 1 mm/sec. Table III is a sample of three weeks of range and range rate biases for June 1984. The date is given as Modified Julian Date (MJD) which is the Julian Date minus 2400000.5, and day of year (DDD), and the number of observations is n. The bias for each pass of tracking data is determined using a Lageos reference orbit derived from laser ranging data. Figure 2 is the residuals from each pass of data. Azimuth and elevation residuals are also given for completeness. The unbiased accuracy of 1 mm/sec (a part in 10^7) is achieved with careful treatment of the tracking system, refraction and the theory of Special Relativity (4). The fact of zero range rate bias is so generally true that we normally do not determine range rate bias, and the range rate bias value in the calibration model is kept at zero. Range rate is therefore the most powerful observable in determining orbits using only the Millstone Radar data. With an accuracy of 1 mm/sec, the range rate is measured to 1×10^{-7} which is comparable with a laser range measurement of 10 cm (10^{-8}).

The situation with azimuth and elevation is similar, but not so promising. Basically, the angle measurements are limited by mechanical devices (encoders) to $0^{\circ}.002$. This is a respectable 4×10^{-5} measurement. The calibration model for the azimuth and

TABLE III
MH CALIBRATION WITH LASER REFERENCE ORBIT

MJD	DDD	$\langle R \rangle$ (m)	n	σ (m)	$\langle \dot{R} \rangle$ (mm/sec)	n	σ (mm/sec)
45854.9	155	-4.6	70	3.0	-1.5	71	1.7
45855.9	156	-7.3	96	1.5	-0.6	96	3.1
45857.9	158	-9.9	25	21.3*	1.7	32	1.2
45859.3	160	-13.5	76	4.1	0.2	75	2.1
45861.3	162	-10.5	70	1.7	-0.2	69	2.1
45863.3	164	-8.9	83	23.8*	0.0	88	1.3
45864.8	165	-8.6	10	1.8	-0.5	9	2.1
45865.2	166	-9.8	98	3.0	1.0	98	2.6
45866.3	167	3.7	104	5.3	1.2	104	3.0
45867.0	168	-8.9	87	3.1	-2.0	88	2.9
45868.4	169	-7.8	60	3.0	-0.0	61	2.8
45870.3	171	-3.7	36	2.3	-1.7	34	1.5
45872.3	173	-13.2	84	3.4	1.1	81	3.8
45873.2	174	-4.9	83	1.8	1.8	72	2.6

* Coded Pulse Data

TABLE IV
AZIMUTH, ELEVATION CALIBRATION MODEL

Calibration Parameter	Dec 1983	February 1984
Azimuth		
bias (mdeg)	-45.0	-45.0
collimation (mdeg)	-12.5	-16.0
Axis-skew (mdeg)	-3.20	-0.333
Elevation		
bias (mdeg)	290.0	293.0
slope (mdeg/deg)	-0.323	-0.347

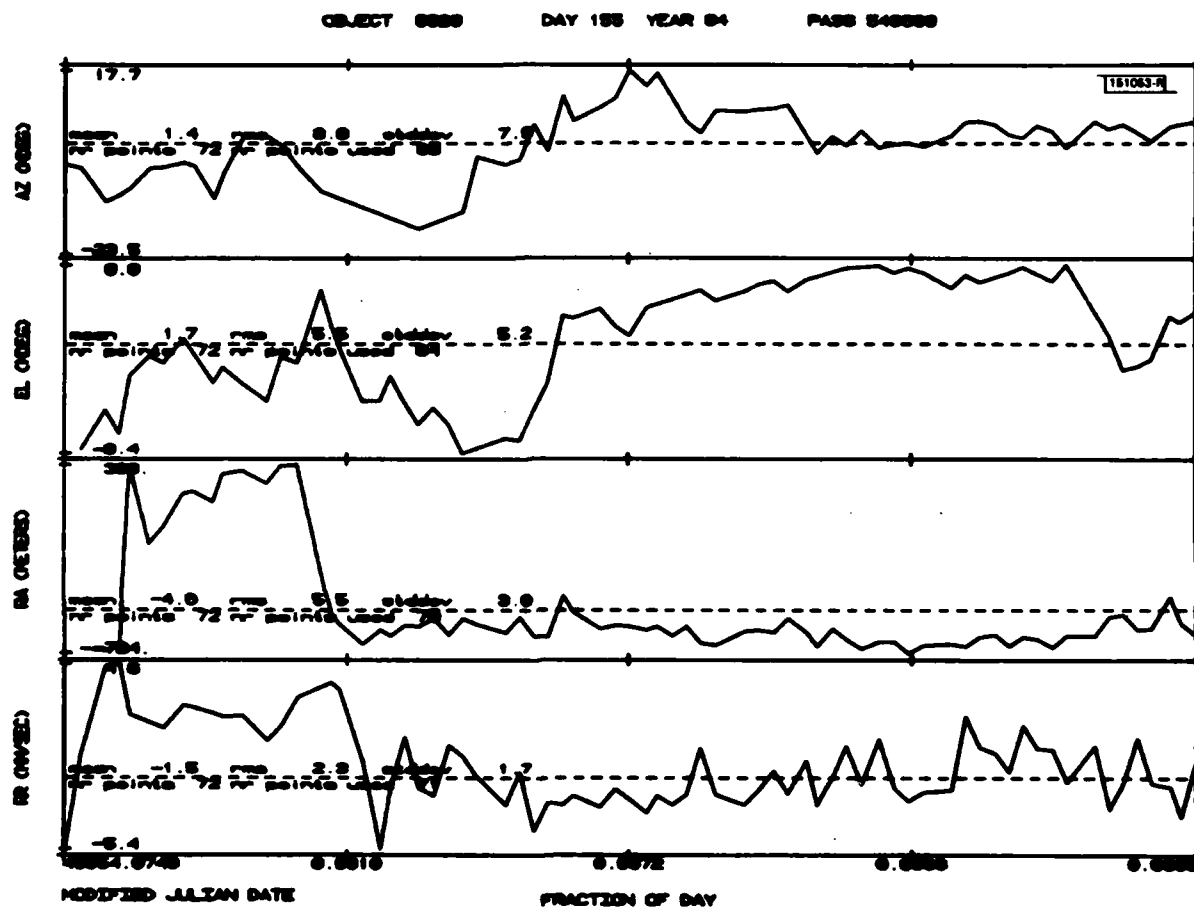


Fig. 2A. Millstone Hill Radar residuals laser reference orbit.

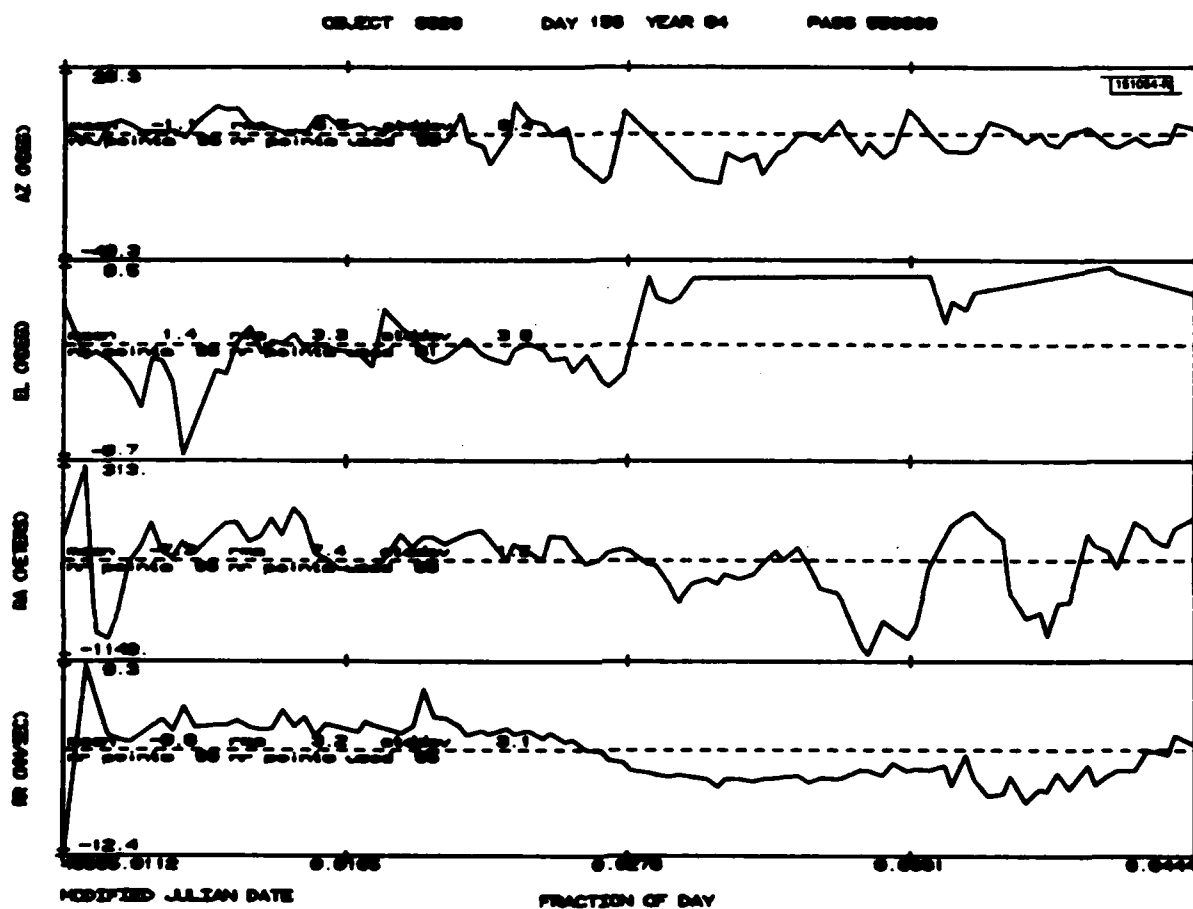


Fig. 2B. Millstone Hill Radar residuals laser reference orbit.

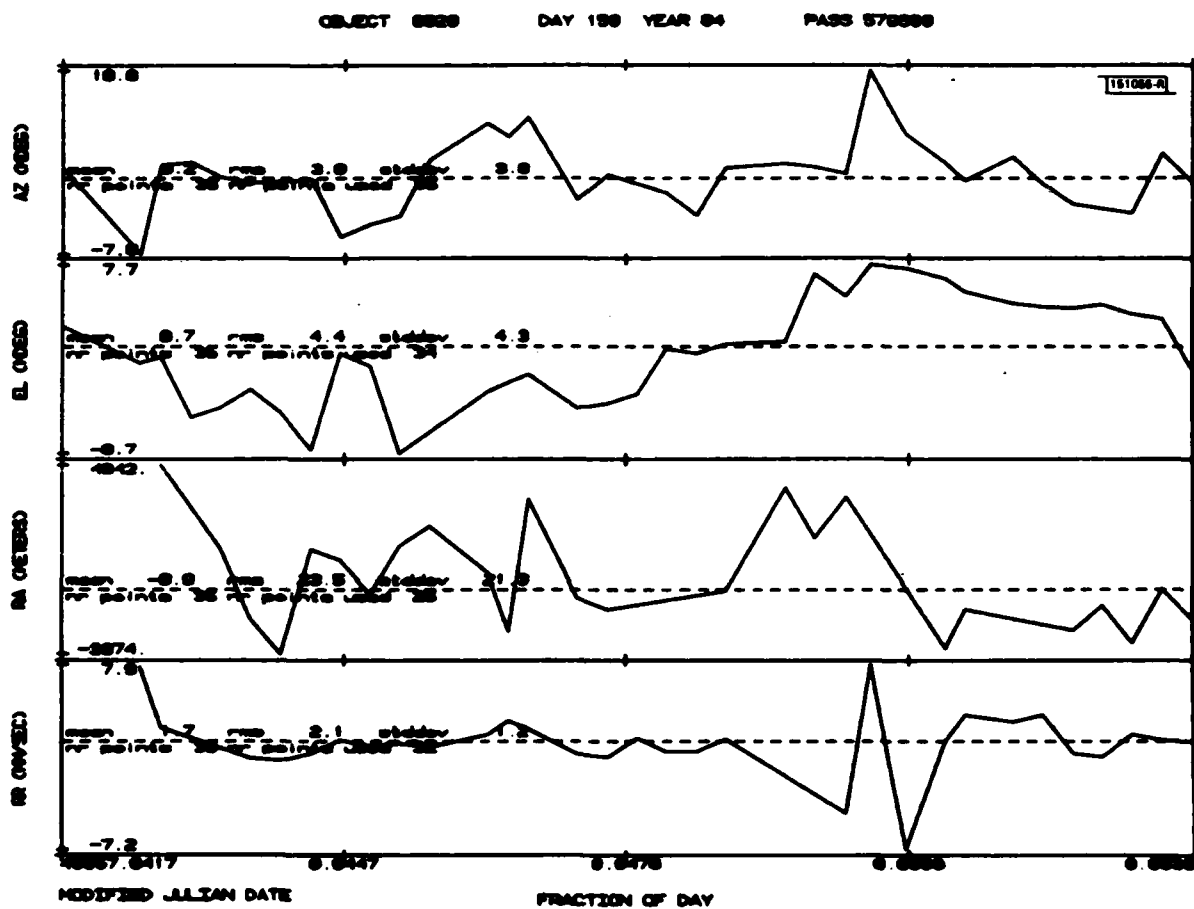


Fig. 2C. Millstone Hill Radar residuals laser reference orbit.

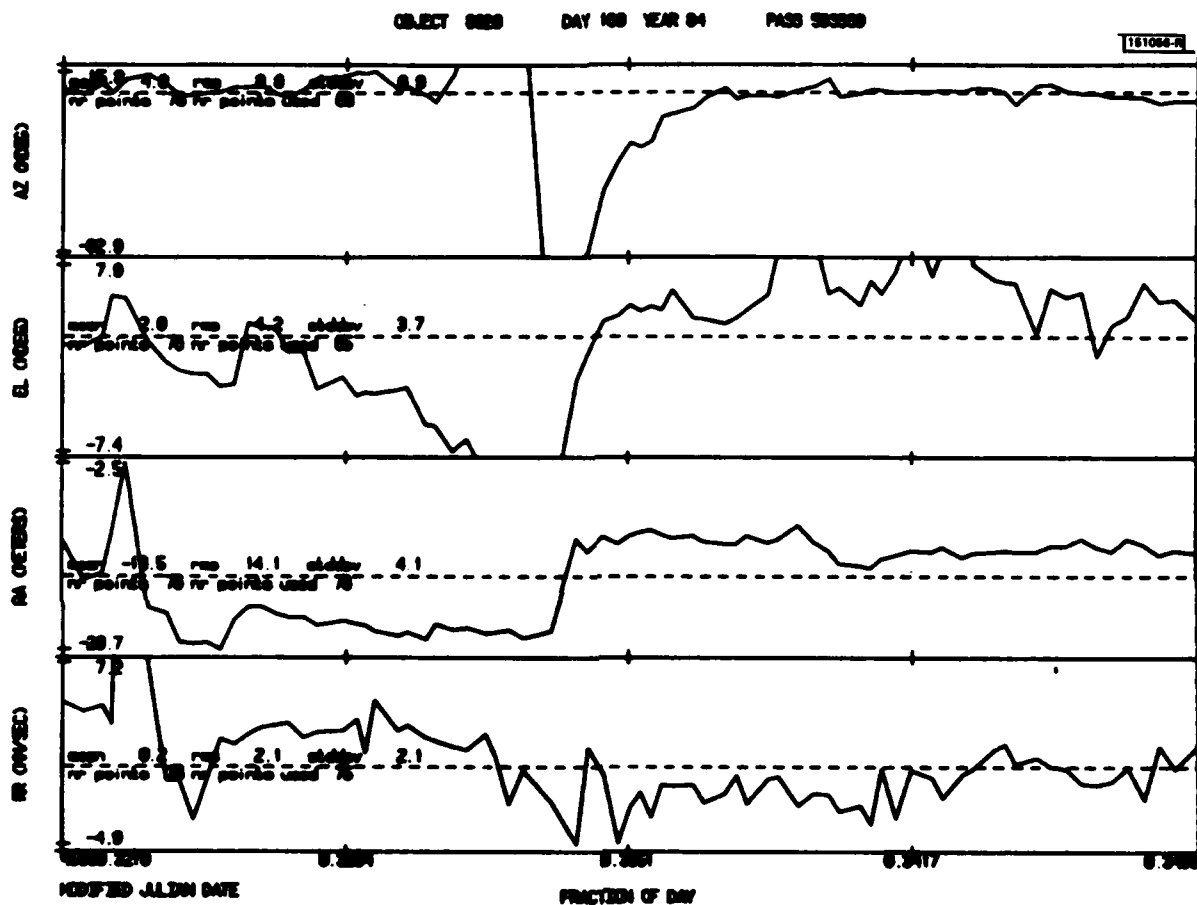


Fig. 2D. Millstone Hill Radar residuals laser reference orbit.

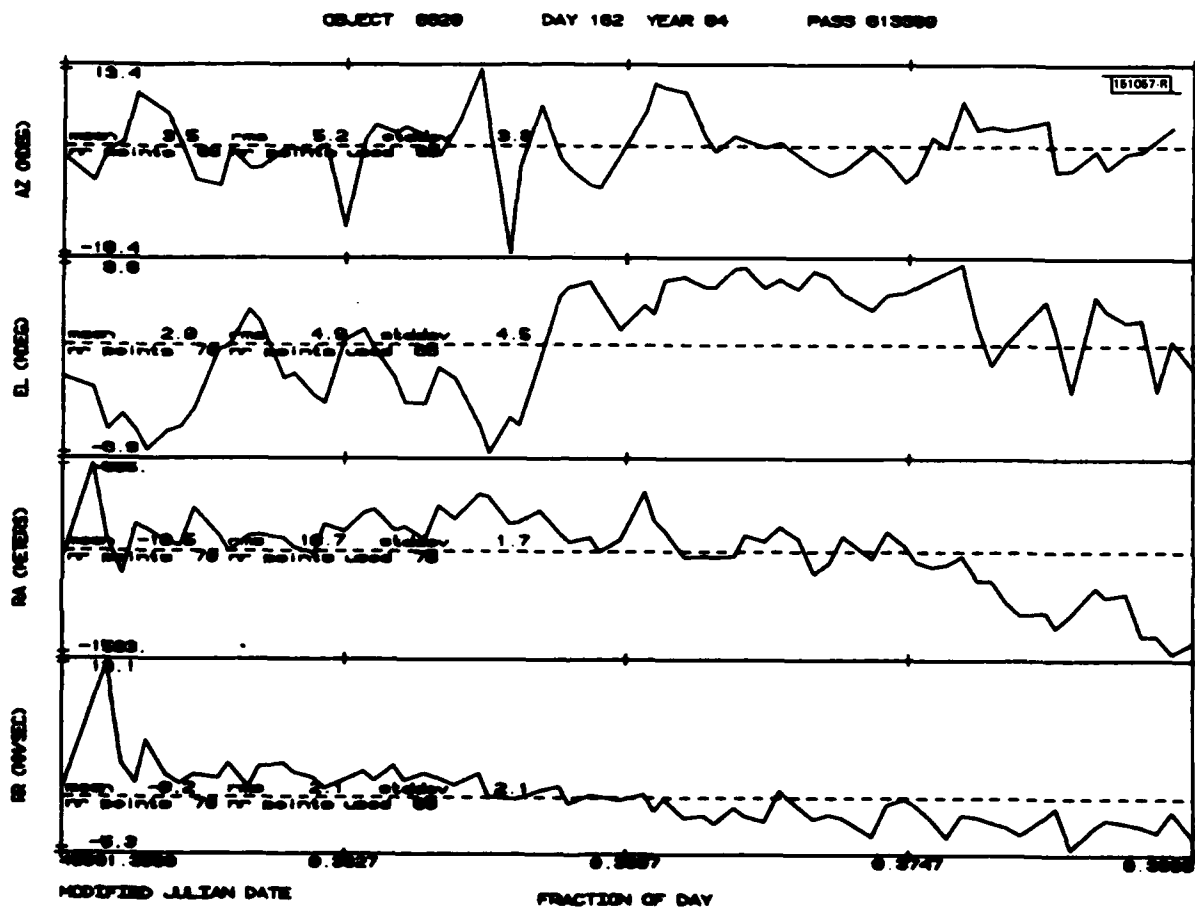


Fig. 2E. Millstone Hill Radar residuals laser reference orbit.

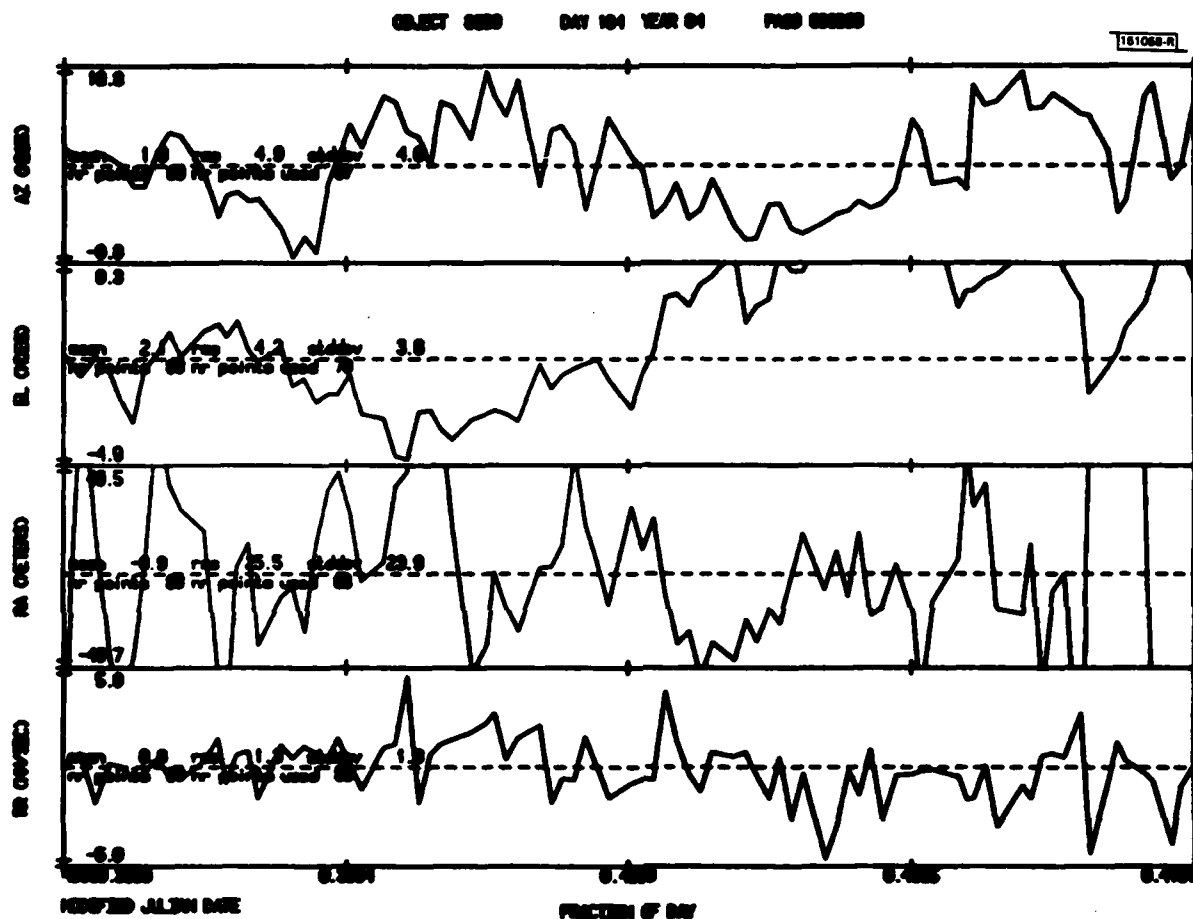


Fig. 2F. Millstone Hill Radar residuals laser reference orbit.

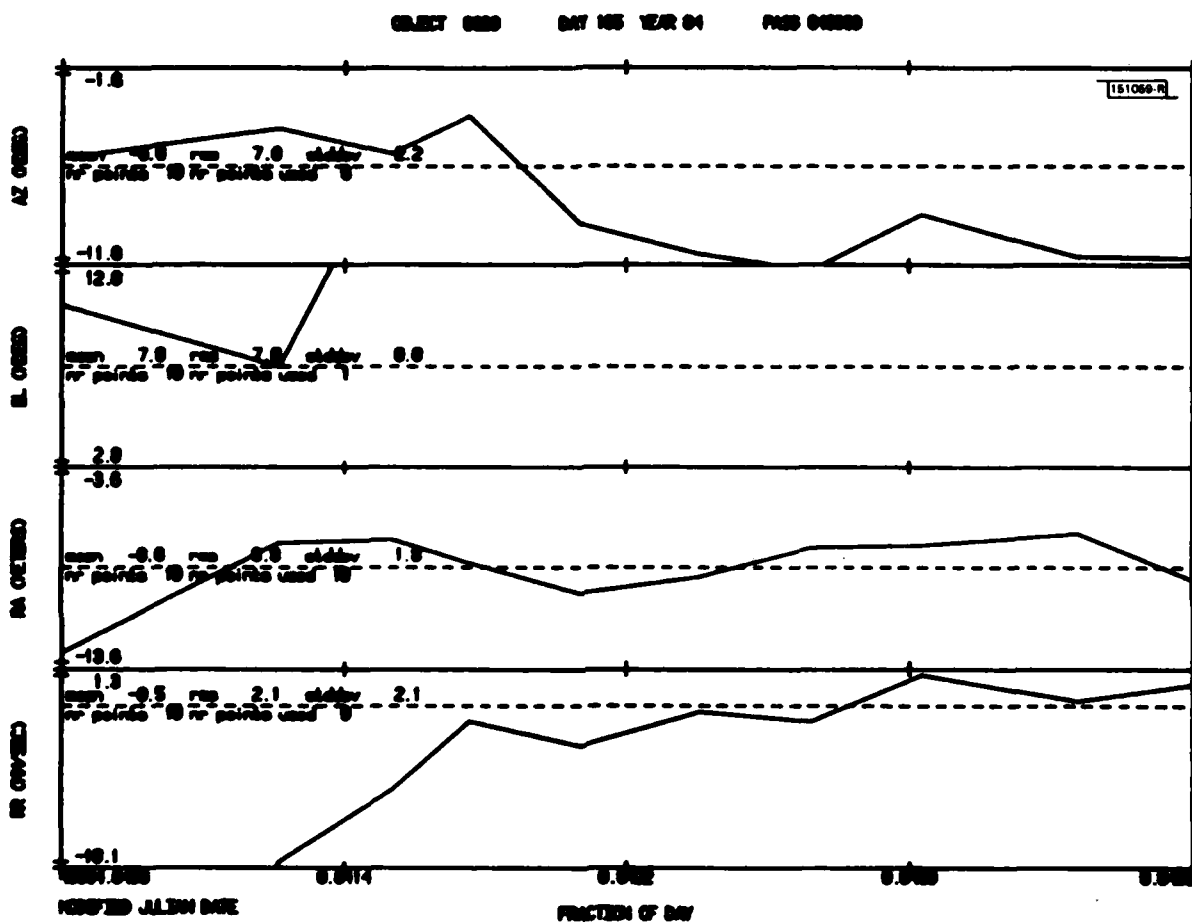


Fig. 2G. Millstone Hill Radar residuals laser reference orbit.

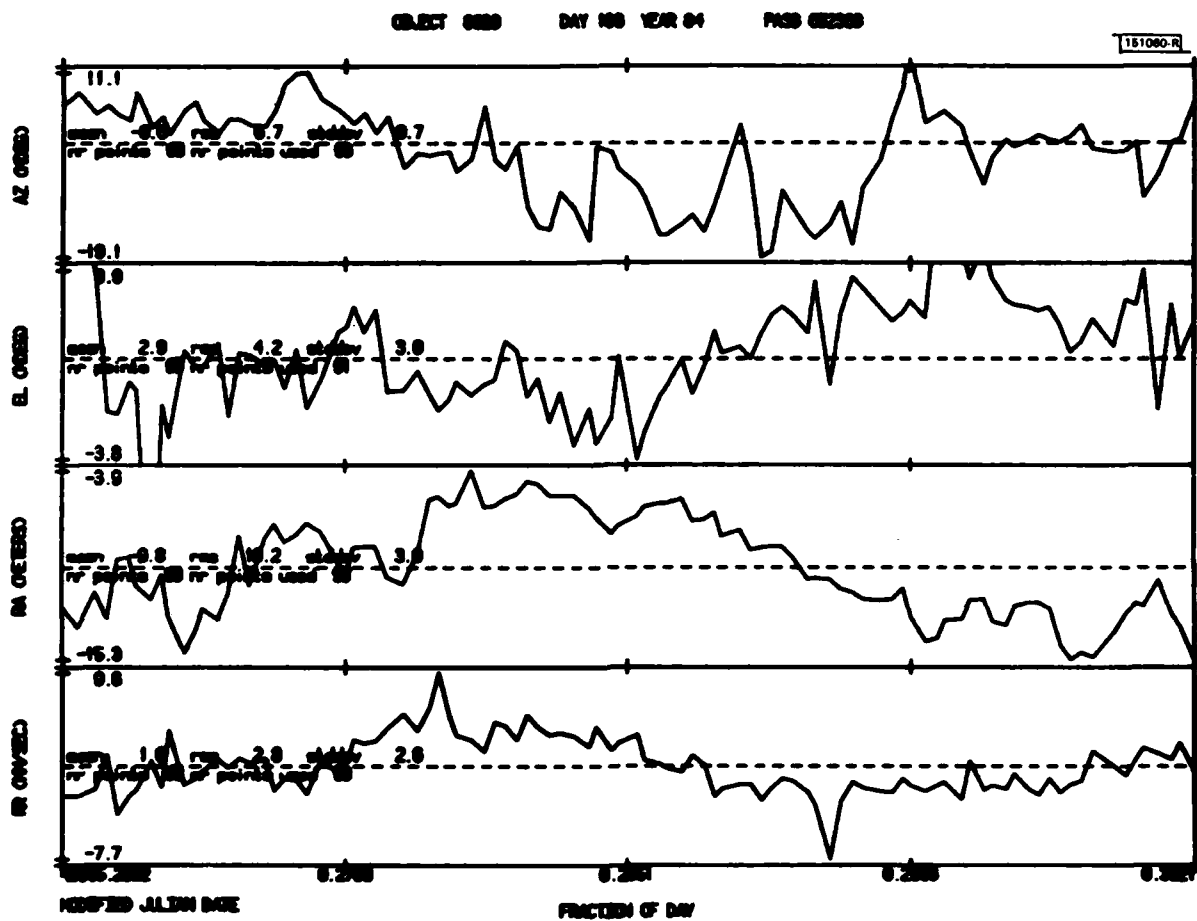


Fig. 2H. Millstone Hill Radar residuals laser reference orbit.

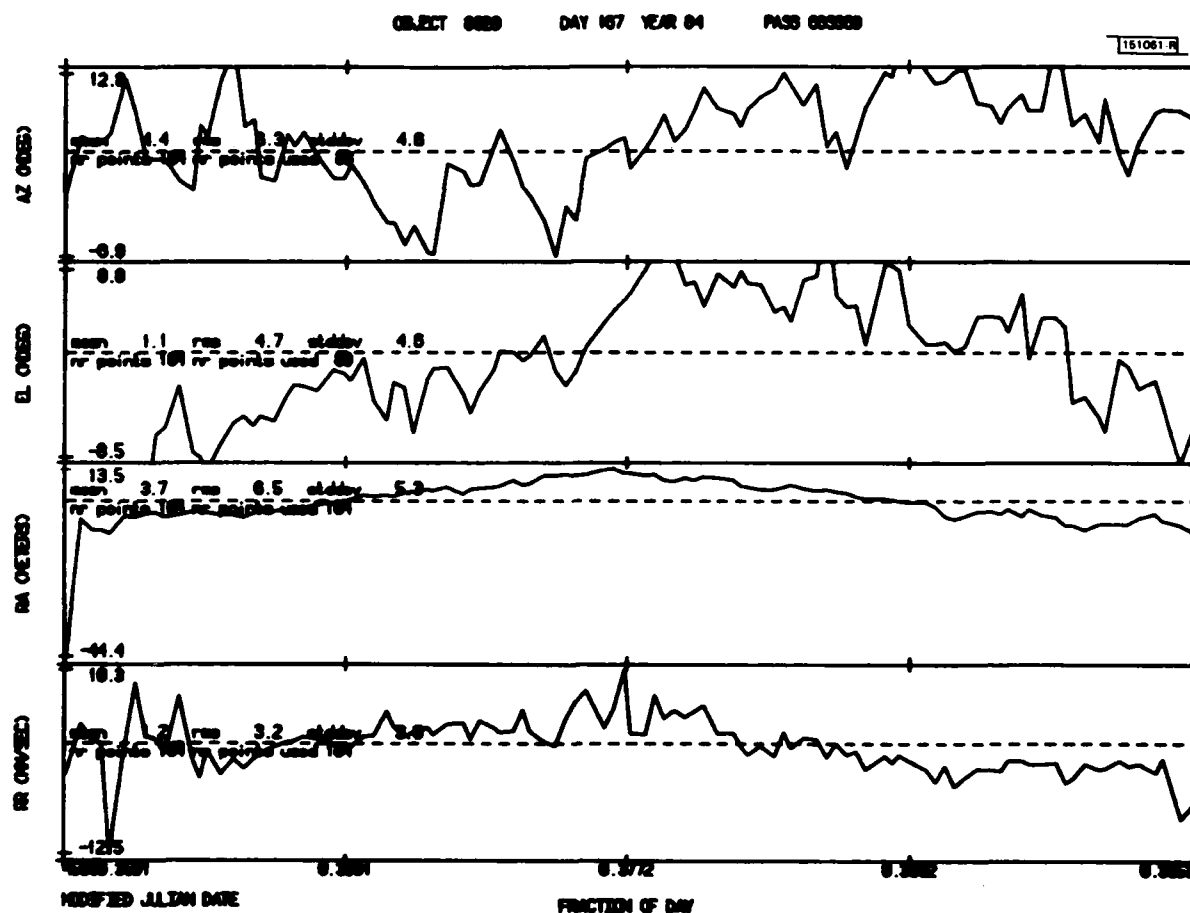


Fig. 2I. Millstone Hill Radar residuals laser reference orbit.

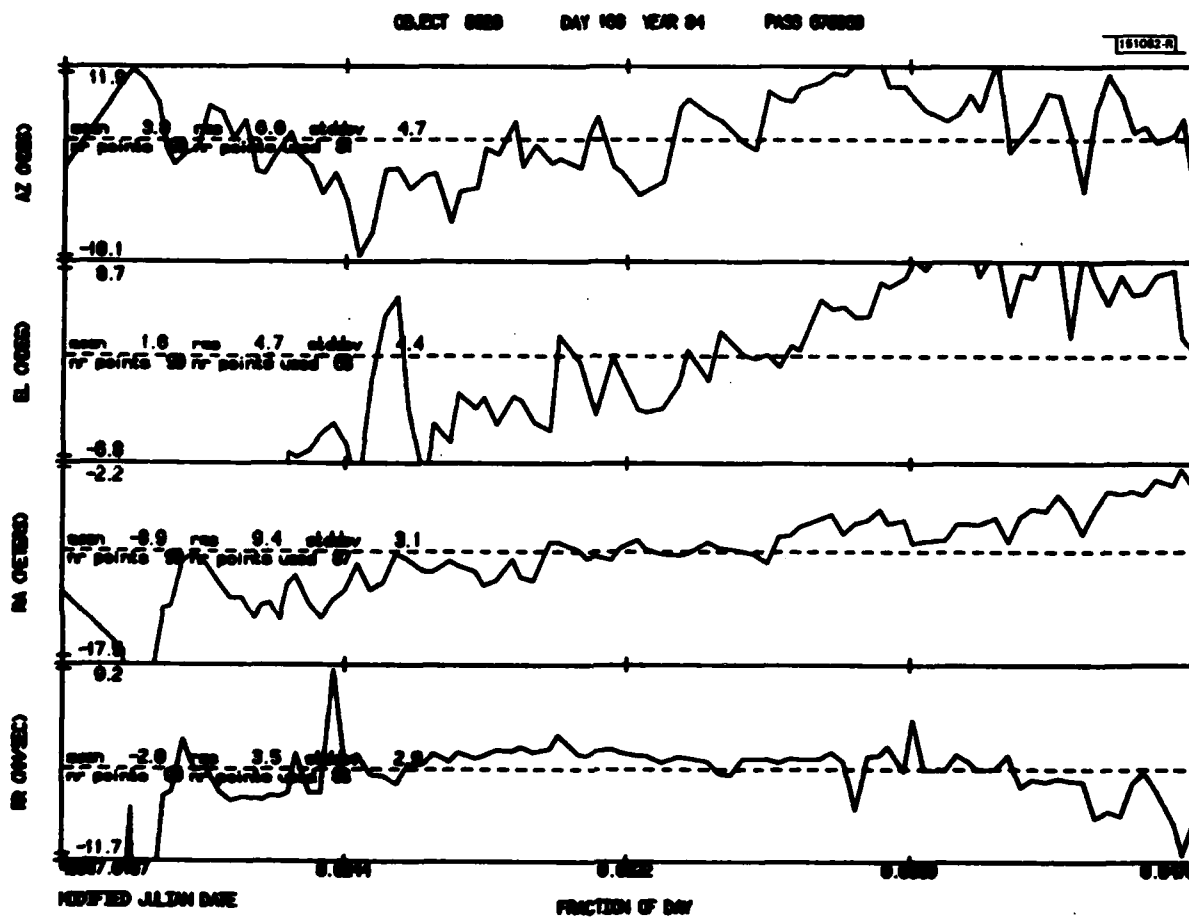


Fig. 2J. Millstone Hill Radar residuals laser reference orbit.

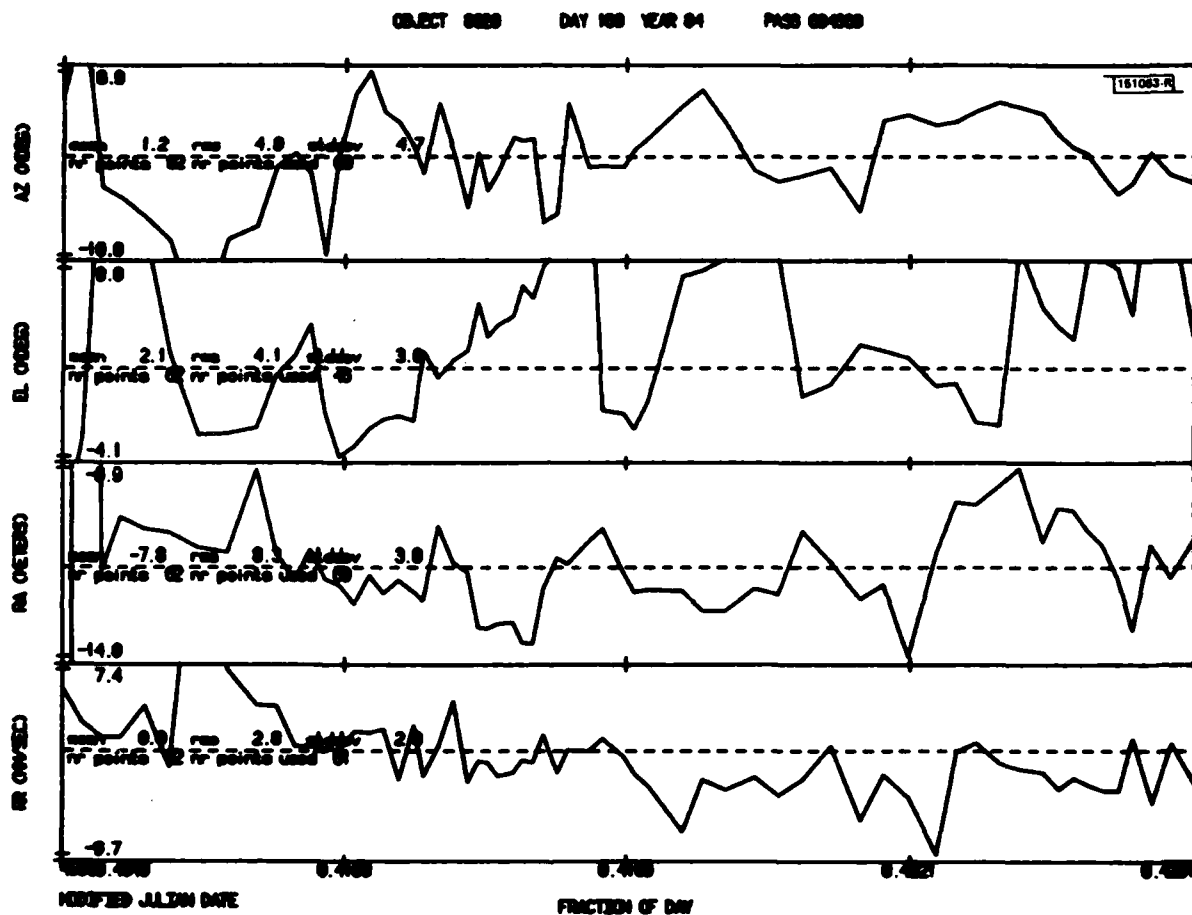


Fig. 2K. Millstone Hill Radar residuals laser reference orbit.

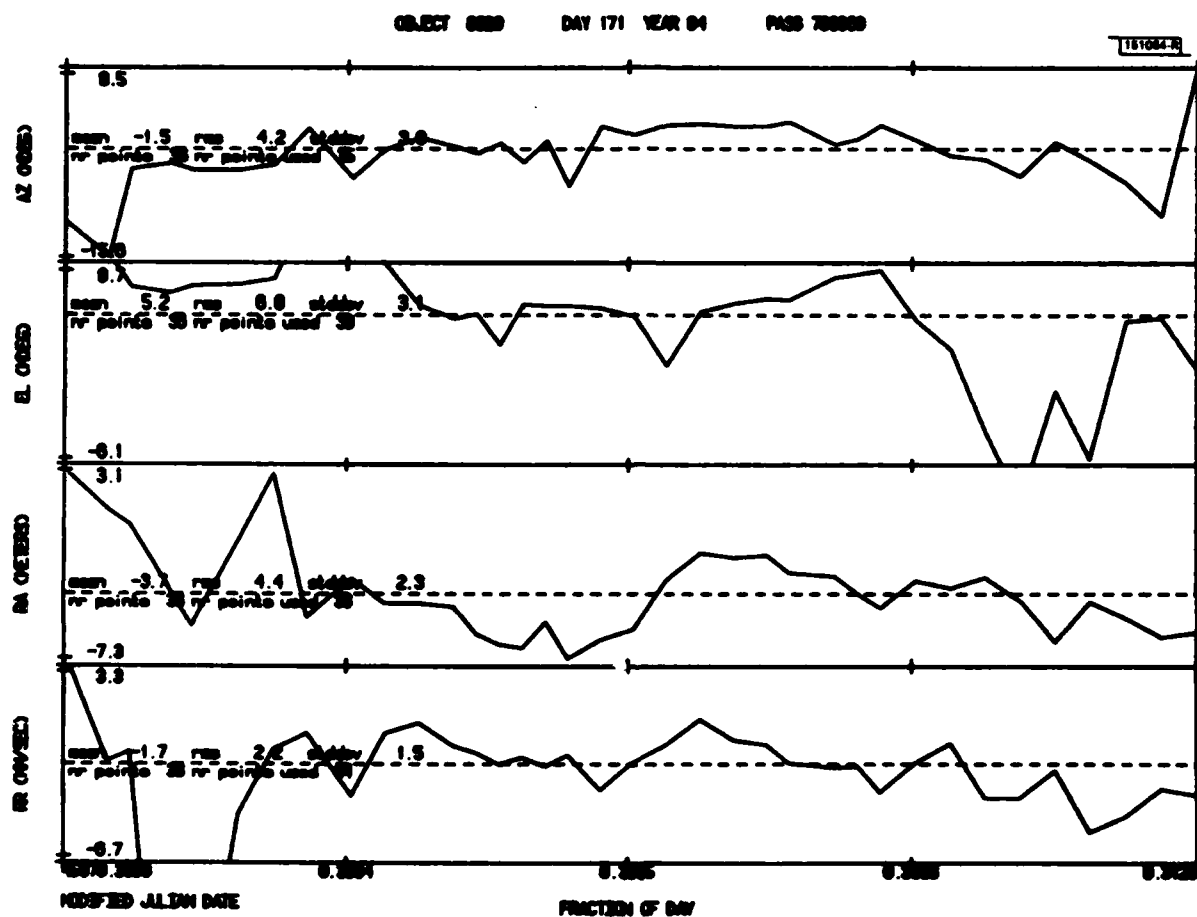


Fig. 2L. Millstone Hill Radar residuals laser reference orbit.

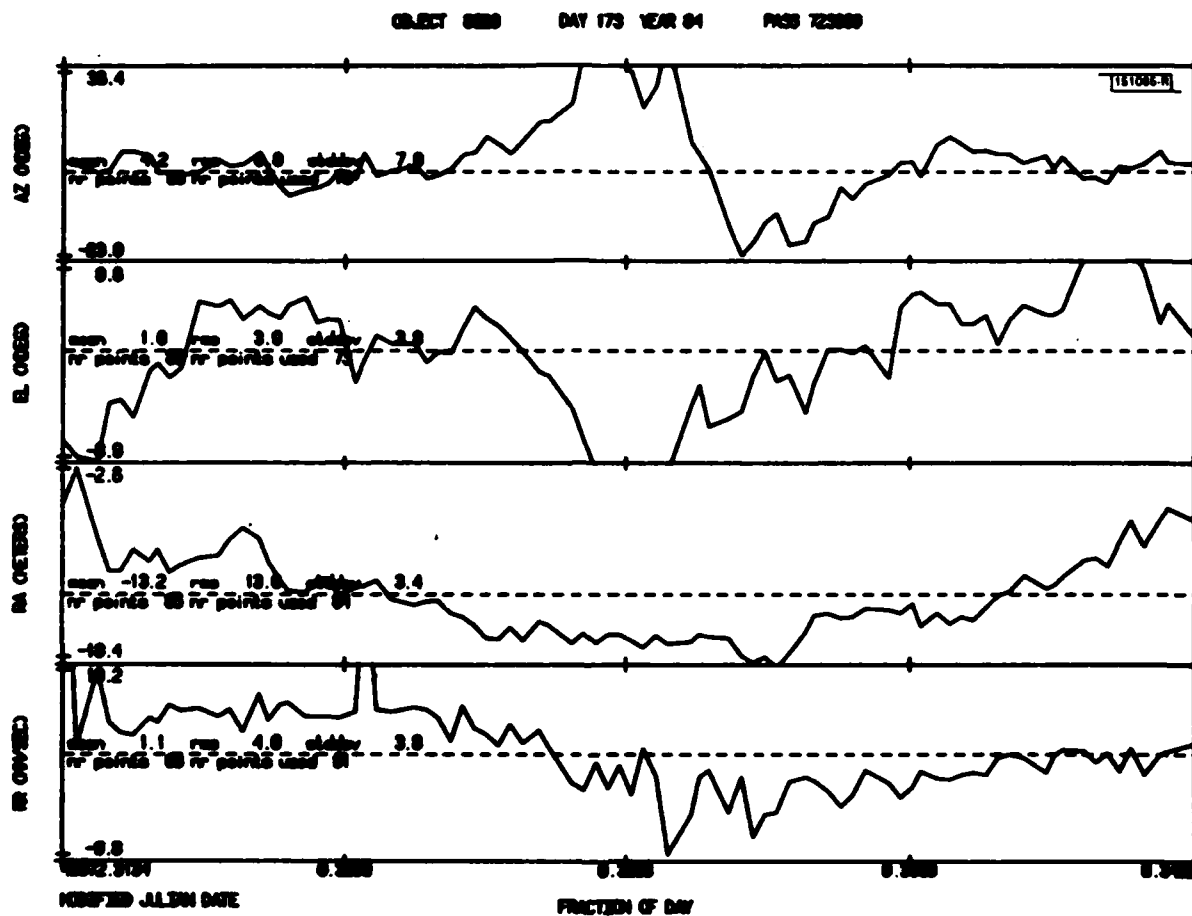


Fig. 2M. Millstone Hill Radar residuals laser reference orbit.

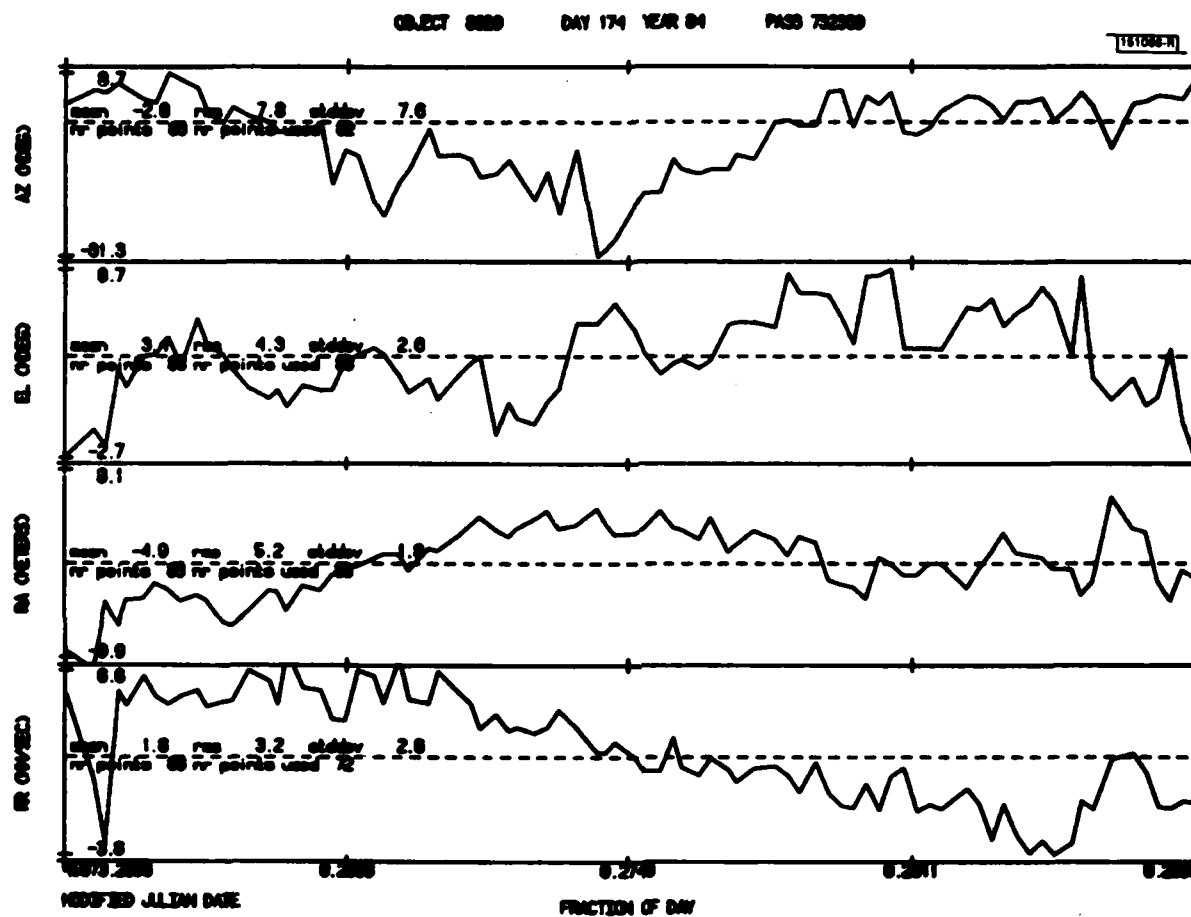


Fig. 2N. Millstone Hill Radar residuals laser reference orbit.

elevation seems stable in the sense that over periods of many months, the parameters have small changes. These changes appear to be seasonal, but too little data is in hand to be sure. As an example, the calibration model adopted in December 1983 and in February 1984 are given in Table IV.

These azimuth and elevation calibration parameters are directly applied to the data going into the metric data base, and therefore, no further correction need to be applied. These parameters are given here for illustration.

There is no evidence that the model parameters for azimuth and elevation are different in the three tracking modes and one would not expect any difference. The situation is made less clear because the angle measurements have not been completely reliable, i.e. a significant number are discarded in any orbital test. This provides less reliable data for establishing calibration parameters, and hence less certain calibration values. Further discussion of angle data is left to another report.

The range calibration for each pass is adequately modelled as a bias. Table III is a sample for three weeks (June 1984) of the bias for each pass determined using a Lageos reference orbit determined with laser ranging data. There is apparently real pass to pass variations in this calibration parameter. Discussion of these data will be given in section 6. Suffice it to say that the bias determination is known to approximately 1 meter: 2×10^{-8} for a synchronous satellite or 1×10^{-7} for Lageos.

5. Refraction

The basic measurement is a two way time delay. The radiation travels at the speed of light in vacuum, and more slowly in the atmosphere or ionosphere, so called refraction. To obtain an estimate of the true range or range rate, we must estimate the contribution of refraction on the observed time delay. The refraction can conveniently be given as a correction to range and range rate.

5.1 Tropospheric Refraction

Many analyses of refraction modeling exist, and the basic relations need not be described (5). We therefore, describe the observed quantities available.

The troposphere extends to about 30km altitude, and for radio frequencies less than the 22.5 GHz water vapor line, is nondispersive; i.e. the index of refraction (n_t) is independent of frequency. Now it is conventional to write

$$n_t = 1 + N_t \times 10^{-6}$$

where N_t is the tropospheric refractivity. The factor 10^{-6} is conventionally included and results in N_t values of approximately 300. For the troposphere, N_t depends on the composition, pressure, temperature, and relative humidity of air. The most commonly used expression for an average atmospheric composition is (5):

$$N_t = \frac{77.6}{T} \left(P + \frac{4810}{T} e \right)$$

where P is the pressure in millibars, T is the temperature in degrees Kelvin, and e is the partial pressure of water vapor in millibars. Since temperature and pressure are not available at altitude, surface data are used for the surface refractivity (N_t^0) and a model with altitude is assumed:

$$N_t(h) = N_t^0 \exp(-h/H)$$

where H is called the scale height. Average values of N_t^0 and H for the United States are approximately 313 and 7km respectively. From the on-site refractometer we monitor N_t^0 . Therefore, calculation of tropospheric refraction assumes the scale height (H) and a plane stratified atmosphere.

5.2 Ionospheric Refraction

The ionosphere consists of ionized particles extending from about 80km to beyond 1000km. There is evidence of charged particles (the plasmasphere) to arbitrary heights, e.g. to 20000km, (6). We must assume, for the moment, that these higher charged particles have a small effect on the total refraction, and ignore them.

The index of refraction (n_i) is less than 1, and is expressed in terms of the ionospheric refractivity as:

$$n_i^2 = 1 - \left(\frac{N_e q^2}{\epsilon_0 M \omega^2} \right) = 1 - \left(\frac{f_0}{f} \right)^2 = 1 - N_i$$

where q is the electron charge 1.6021×10^{-19} coulomb/electron
 M is the electron mass, 9.1091×10^{-31} kg/electron
 ϵ_0 is the permittivity of free space
 $1/(4\pi \times 10^{-7} \text{c}^2) \approx 10^{-9}/(36\pi)$ farad/m
 N_e is the electron density (electrons/m³)
 f is the frequency of the propagating wave ($2\pi f = \omega$)(Hz)
 f_0 is equal to $8.978/\sqrt{N_e}$ is called the plasma frequency
 c is the speed of light $c = 299792458$ m/sec.

Since n_i depends of frequency (ω), the ionosphere is dispersive. Now, if $\omega < \omega_0$ n_i cannot be real and no wave will propagate, i.e. there will be total reflection. For typical values of N_e , $\omega_0 \approx 10$ MHz. Therefore the L-Band (1295MHz) and UHF (400MHz) frequencies are well above the plasma frequency.

With an ionosonde or backscatter radar, one transmits a number of frequencies. Those frequencies below ω_0 , are all reflected. Measuring the delay of the reflected wave at any frequency, gives an estimate of the height of the electron concentration corresponding to that resonant frequency. The maximum frequency reflected, therefore corresponds to the maximum electron density (N_{\max}) and is known as $f_0 F_2$. Now, for calculation of refraction in range and doppler measurements, one

needs the integrated electron content or Total Electron Content (TEC) along the propagation path. We have no way of knowing this from the bottom side ionosonde measurements since they tell us nothing about the distribution of electron density above h_{\max} , the height of the maximum electron density. Neither does it indicate anything about the thickness of the ionosphere. It is possible to use a general model of the ionosphere and employ the observed maximum electron density to scale the model. It is found (7) that the slab thickness $S = \text{TEC}/N_{\max}$ is rather stable and well behaved. It is more easily modeled than either TEC or N_{\max} , and we use the relation that

$$\text{TEC}(\text{instantaneous}) = N_{\max}(\text{measured}) \cdot S(\text{model}).$$

Therefore, based on these arguments (7) we use a slab model of the ionosphere:

$$N_e = \begin{cases} 0 & h < h_{\max} \\ 1.24 \times 10^{10} f_0 F_2 & h_{\max} < h < h_{\max} + S \\ 0 & h < h_{\max} + S \end{cases}$$

which is equivalent to modeling the index of refraction as

$$N_i^2 = \begin{cases} 1 & h < h_{\max} \\ 1 - (f_0 F_2 / f)^2 & h_{\max} < h < h_{\max} + S \\ 1 & h < h_{\max} + S \end{cases}$$

where S is the slab thickness, $f_0 F_2$ is given in MHz and N_e in electrons m^{-3} .

5.3 Refraction Corrections

The index of refraction (n) allows one to calculate the transmission time of electromagnetic waves from the propagation velocity (v), noting that

$$v = c/n$$

where c is the speed of light in vacuo. Strictly, this is the phase velocity (v_p). For a nondispersive medium like the troposphere $v_p < c$, and v_p is the same as the group velocity (v_g) and the signal velocity (v_s). We have the time of transit from location x_1 to location x_2 as:

$$\tau = \int_{x_1}^{x_2} \frac{dx}{v} = \frac{1}{c} \int_{x_1}^{x_2} n \, dx.$$

For a dispersive medium, such as the ionosphere, the result depends on the type of measurement. In the ionosphere the phase velocity $v_p = c/n_i > c$. However, the group velocity $v_g = v_p - dn/d\omega < c$. Note that for this dependence of n_i on ω we have $(v_g v_p) = c^2$. Now for measurements involving the group velocity we have:

$$\tau_g = \int_{x_1}^{x_2} \frac{dx}{v_g} = \frac{1}{c} \int_{x_1}^{x_2} (1 + (1/2)N_i) \, dx$$

and for measurement involving the phase velocity we would have:

$$\tau_p = \frac{1}{c} \int_{x_1}^{x_2} (1 - (1/2)N_i) dx.$$

Now, one cannot measure τ_p , but it is possible to measure phase differences. Conceptually the difference in phase, $\Delta\phi$, between the return signal and the local oscillator, measured in successive pulses separated by Δt can give the doppler shift:

$$\Delta f_i = \frac{\Delta\phi_i - \Delta\phi_{i-1}}{\Delta t}$$

Now using approximations sufficient for elevations greater than 10 degrees, the additional delay due to refraction, expressed in meters for the troposphere is:

$$\Delta r_t = 7 \times 10^{-3} N_t / \sin E$$

where E is the elevation angle, and for the ionosphere, using the group velocity, is:

$$\Delta r_i = \frac{1}{2} \left(\frac{f_0 F_2}{f} \right)^2 S \sec x$$

where x is defined by

$$\sec x = \frac{R_0}{\sqrt{R_0^2 - R_e^2 \cos^2 E}}$$

E is the elevation

R_e is the geocentric station radius

$R_0 = R_e + h_{\max}$ is the geocentric height of the maximum electron density and

S is the slab thickness.

The values of f_oF_2 are measured with a local ionosonde, and h_{max} and S are computed from models by (7). These models are functions of solar activity (sun spot number in terms of the 10.7 cm solar flux), time of day and season. In case N_t or f_oF_2 are not observed, seasonal estimates of them are used.

The correction to range rate for the troposphere is:

$$\Delta \dot{r}_t = \frac{-7 \times 10^{-3} N_t \cos E}{\sin^2 E} \frac{dE}{dt}$$

and for the ionosphere, using the phase velocity is:

$$\Delta \dot{r}_i = \frac{1}{2} \left(\frac{f_oF_2}{f} \right)^2 S \sec^3 x \left(\frac{R_e}{R_o} \right)^2 \cos E \sin E \frac{dE}{dt}$$

The range-rate measurement from the frequency domain tracker at Millstone Hill is based on the difference in phase, and hence the correction depends on the phase velocity. For the time domain tracker, it depends on the group velocity, and the correction has the opposite sign.

As an example, the size of the refraction corrections are estimated as follows: Typical values of the troposphere are $N_t=313$. Therefore we have

at zenith	$E=90^\circ$	$\Delta r_t = 2.2 \text{ m}$
and at	$E=20^\circ$	$\Delta r_t = 6.4 \text{ m}$

For the ionosphere with

$$f_0 F_2 = 12 \text{ MHz}$$

$$f = 1200 \text{ MHz (L-band)}$$

$$S = 280 \text{ km}$$

$$h_{\text{max}} = 300 \text{ km}$$

$$R_0 = 6678 \text{ km}$$

we have:

Elevation (°)	x (°)	Δr_i (m)
90	0.	14.
20	63.8	32.

and with the same assumptions as before, we have for the ionosphere at $E = 20^\circ$

$$\dot{\Delta r}_i = 1.5 \text{ cm/sec.}$$

An example of ionospheric and tropospheric refractions is given in Fig. 3.

The troposphere correction should be accurate to a few percent. The ionosphere correction is based on a framework of assumptions and approximations. It is clear that the slab model is a significant oversimplification of the actual ionosphere. It is expected to be no better than 25%. During periods of quiescent ionosphere, i.e. away from day night transition and solar disturbance, this model should be better than 10%. During

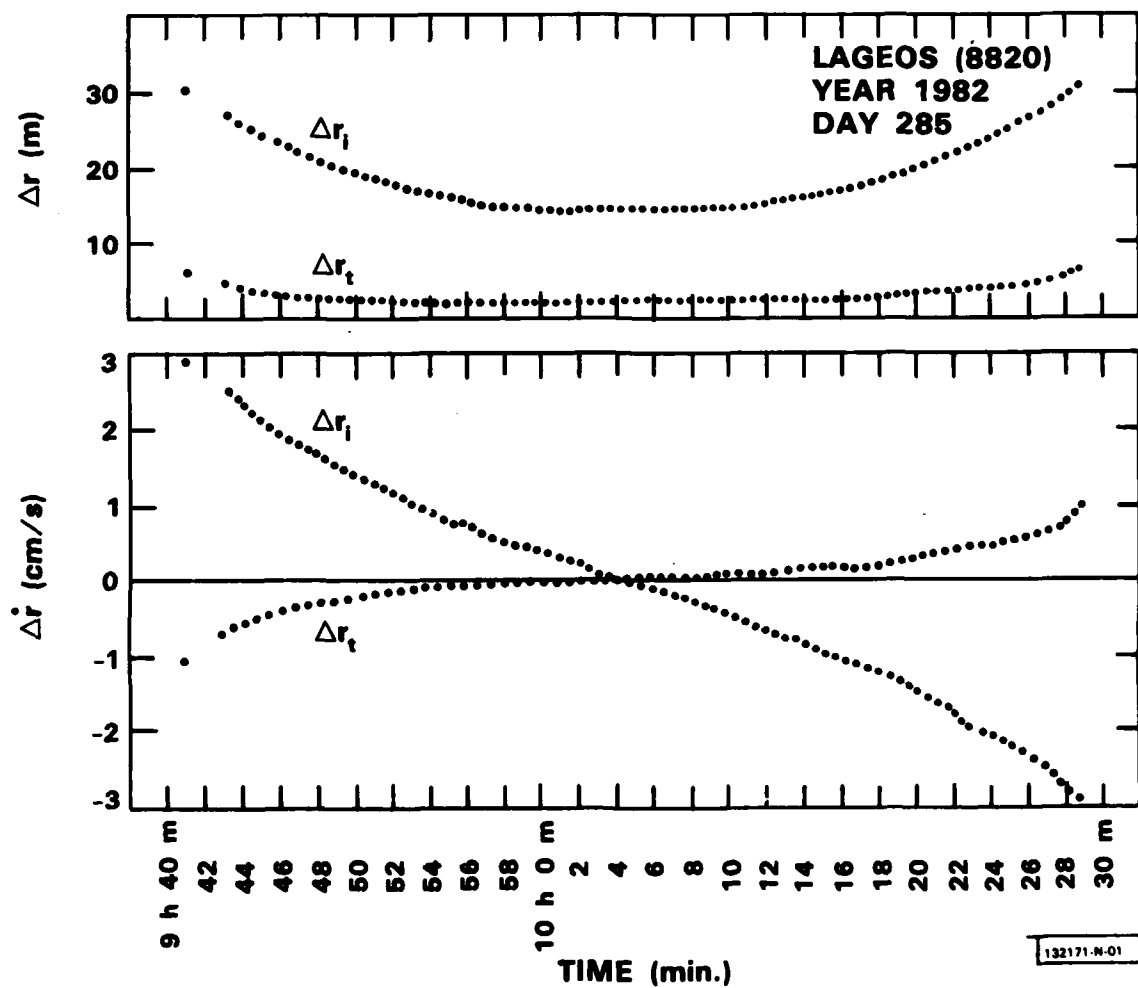


Fig. 3. Ionospheric (i) and tropospheric (t).

periods where the auroral trough extends to the latitude of Millstone Hill it could be considerably worse (8). This ionospheric model works remarkably well most of the time. There seems little evidence of unmodeled refraction in the orbital residuals. It should be kept in mind that during the last year solar activity has been relatively low and the ionosphere has consequently been relatively well behaved. Therefore, the ionospheric correction has been smaller than usual. The main lesson is that further advances in system accuracy will certainly require better modeling and monitoring of the ionosphere and troposphere refraction.

6. Orbital Results

The basic orbit computation program is a numerical integration, with variable step size, automatic truncation and round off error control. The force model used is described in Table V, and the reference system is described in Table VI. The orbital fit to laser ranging data is not yet at the accuracy of the data; however for the radar data the orbit accuracy does exceed the data accuracy.

For analysis of Millstone Radar Data alone, the parameters described in Tables V and VI can be used directly for orbit determination. The error committed in this way is less than the observation uncertainty. However for the precision laser range data, this is not true. In particular the following quantities must be determined with each trajectory (typically 8 days duration):

- 1) Drag Parameter
- 2) Earth Polar Motion
- 3) Earth rate of rotation.

In addition there may be laser data from new stations whose coordinates are not so well known. In this case, the solution is improved by including the three station coordinates in the solution vector. Therefore, typical laser data runs have as solution parameters: 6 orbital constants + drag acceleration + 3 earth rotation parameters + 3 station coordinates.

Table V
Force Model

Geopotential	GEML2 to degree and order 20 (9)
sun & moon	USNO Lunar Ephemeris (10)
Body Tides	$k_2 = 0.285$ $\epsilon = 0.0^\circ$
Solar Radiation Pressure	$K = 1.002$
Earth Albedo	$\alpha = 0.32$
Drag	$\rho_0 = 3.43 \times 10^{-19}$ grams/cm ³
General Relativity	$\gamma = 1.0$

Table VI
Reference Frame

Precession & Nutation	IAU J2000 System (10)
Polar Motion and UT1	BIH Rapid service, USNO Predictions and Determined with Laser Data
Station Coordinates	Laser Site coordinates (11)
Tide displacement	$h = 0.60$

When sufficient data from a new station is available, reliable coordinates can be determined, and that site can be held fixed. Figure 4 shows the range residuals for a pass from Millstone, and the range residuals from an overlapping pass of laser ranging data. This is a good, but typical, result from an 8 day orbit fit. On Fig. 4 are listed additional solution parameters and their formal uncertainty.

The drag parameter, polar motion and earth rotation data are real, time dependent, geophysical information, uniquely provided by laser ranging to Lageos. These geophysical data will be discussed elsewhere.

The accuracy of the Lageos orbit fit using quick look laser ranging data is at present 50 cm r.m.s. This is due to lack of final calibration and editing of the laser data, and the preliminary coordinates used for some of the stations. The accuracy of the Lageos orbit fit using Millstone radar data is 2 to 5 meters r.m.s. The larger error occurs when the amount of data decreases. For extrapolation, (modes 2 and 4) the errors grow to 1 m and 10 m for the laser derived and radar derived orbits respectively.

The determination of Range Bias has been made using mode 1 since December 1983. The values are given in Appendix A and are plotted in Fig. 5. These values are corrections to the nominal calibration model used for data in the Metric Data Base.

Therefore these values can be used to correct data in the metric data base. This correction can be applied to any satellite observed during the same tracking session with the same tracking mode. For each entry the date is given in three ways:

1) Modified Julian Day ($MJD = \text{Julian Date} - 2400000.5$) to 0.1 days, 2) calendar date, and 3) day of year. The range correction is given in meters. The number of orbit fits containing the pass of data and an uncertainty are also given. When the number of estimates is two, the value given is the mean, and the uncertainty is half the difference. For more than two estimates, the mean is given and the uncertainty is the root mean square difference from the mean. Also given, when available, is the range bias derived from a reference orbit computed from laser ranging data. A recent history of the radar operation is evident from this figure, and the annotations. For example, the change in calibration accompanying installation of a new transmitter component is dramatic. The rapid detection and consequent change of the nominal calibration model was possible because of the routine use of Mode 2 calculation of range bias.

These calibration data are strictly for the frequency domain 1 MHz chirped tracker. The calibration correction given in appendix A can be added to data in the metric data base for any satellite taken with the frequency domain tracker during the same tracking session. Range data corrected in this way can be

considered to have an accuracy associated with the bias value used i.e. 2 to 5 m. This has been done with success for a number of investigations.

There are some tracks taken with the experimental 1 MHz time domain tracker. The range bias values are consistent, but significantly different from the others in the time period. Apparently the time domain tracker is not consistent with the frequency domain tracker from the range calibration stand point. More data are required. Clearly it is desirable for the two trackers to have the same calibration; the frequency domain tracker calibration result can then be applied to the time domain tracked data, and only one calibration model need be maintained.

It must be emphasized that this calibration result does not apply to the so called coded pulse data. The coded pulse data is a narrow band alternative tracking mode. The signal to noise ratio for Lageos results in range precision of 80 to 120 meters. At present it is used during the acquisition phase of all passes and a number of points observed this way are in the metric data base. It can also be true that a whole pass is taken in coded pulse mode. However so little data is available on Lageos, that nothing can be said about the calibration of the coded pulse data.

A small number of tracks were taken with the correlator mode rather than the array processor mode. There is strong

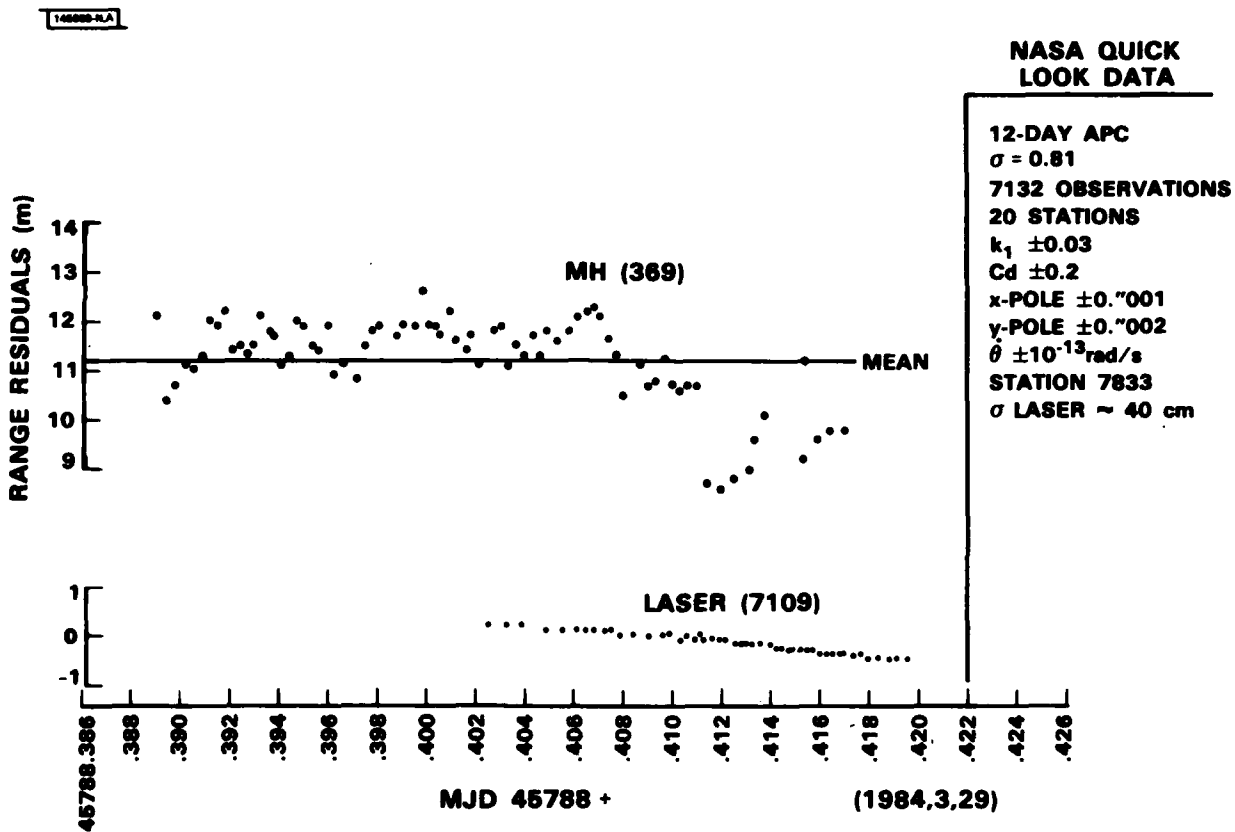


Fig. 4. Orbital residuals.

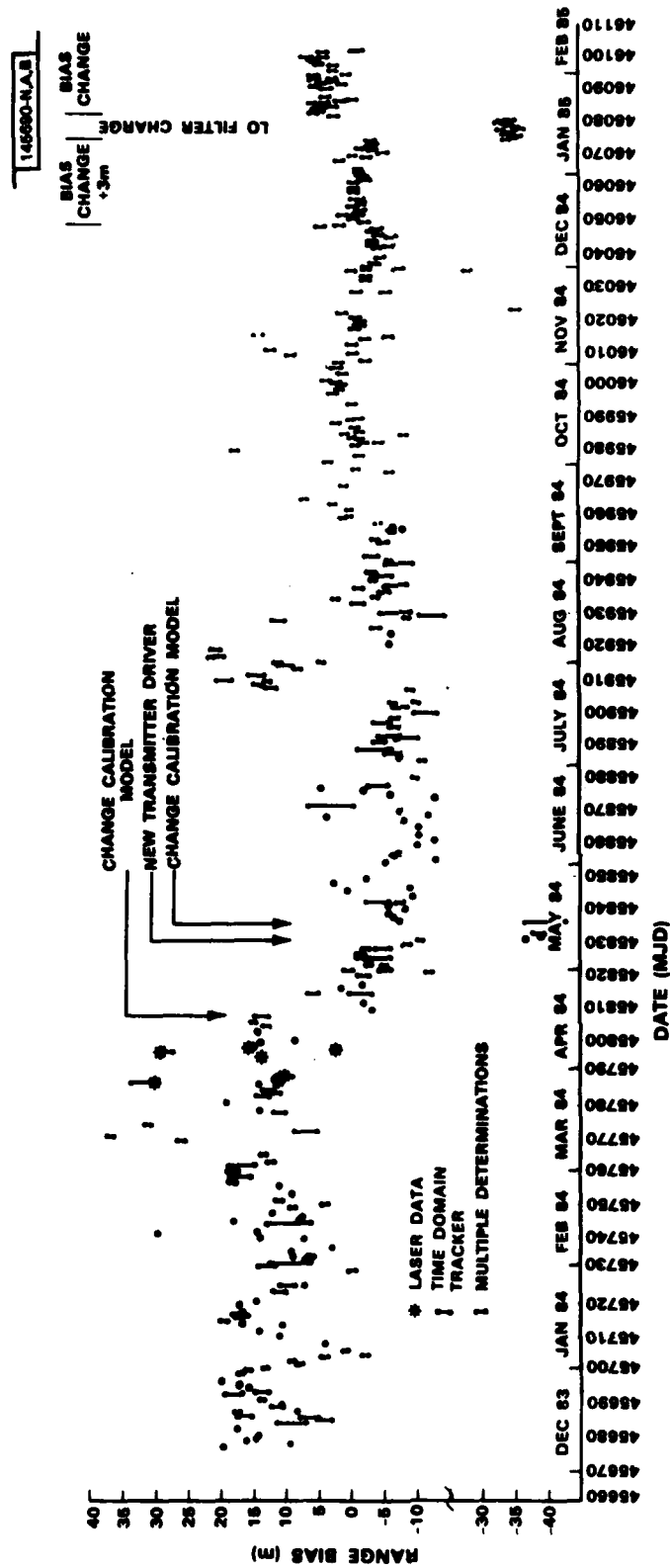


Fig. 5. Range calibration Millstone Hill Radar.

evidence of roughly, a 15 m bias introduced using the correlator. To demonstrate this a track was taken, where the tracking mode was switched in mid pass from correlator to frequency domain, and then to time domain tracking. The range residuals are plotted in Fig. 6, which illustrates two points. First, the frequency domain tracker with the correlator has a 15 meter bias, with respect to the frequency domain tracker and the time domain and frequency domain trackers have appear to a different range calibration bias.

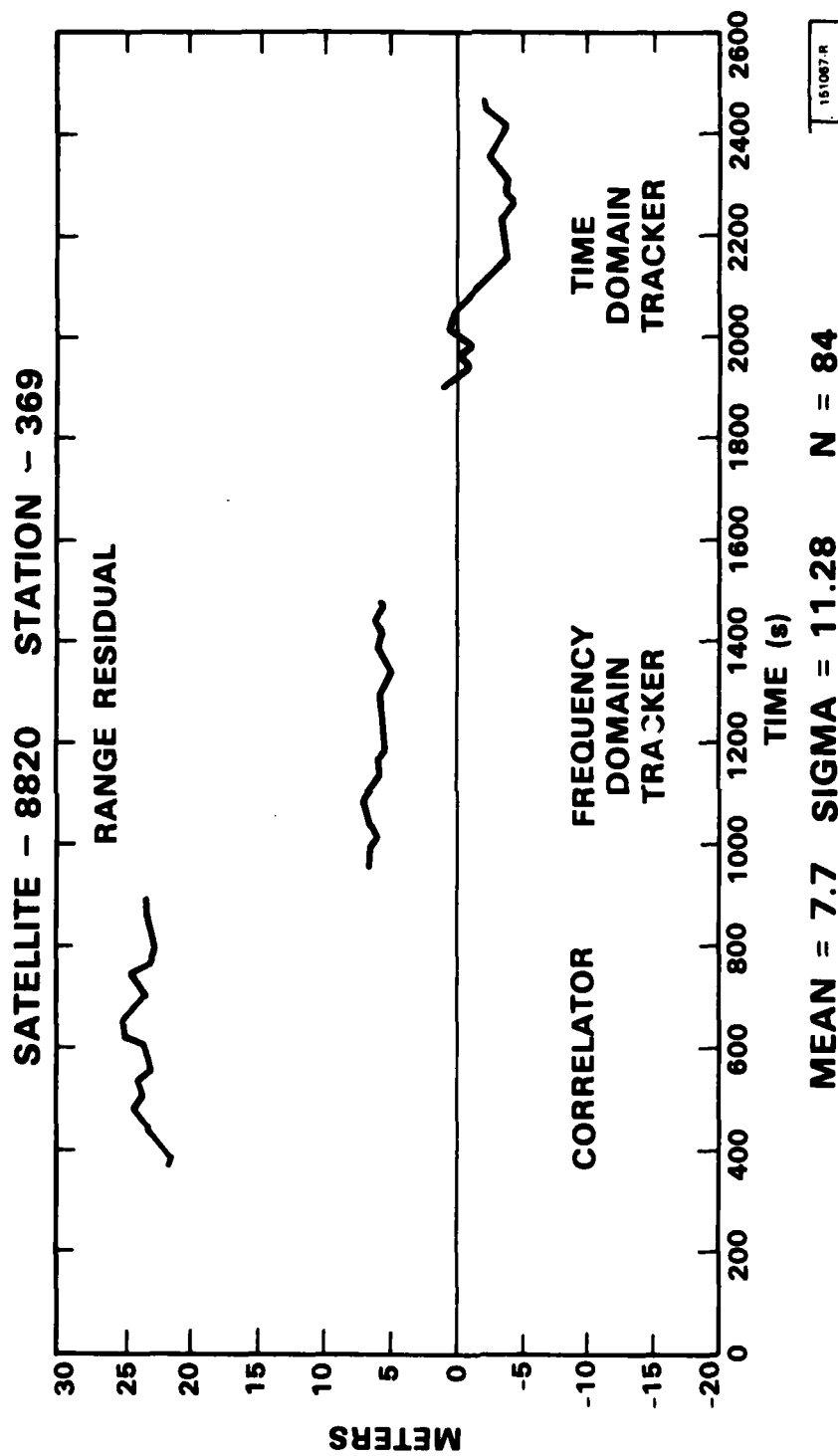


Fig. 6. Residuals for correlator, frequency domain, and time domain tracking.

7. Prediction Accuracy

The results reported here are essentially from an a posteriori analysis. To move to Mode 2 or Mode 4 operation, which would provide more immediate calibration values, requires predictions of the satellite position and the earth's position. As mentioned above, precision orbit determination requires simultaneous determination of the satellite state vector and a number of time variable geophysical parameters. The geophysical parameters that most stress the system are the "along track" drag like force and the UT1. The variability of both of these is apparently due to meteorological effects and are not easily predictable. We give in Fig. 7 the along track acceleration recovered from the laser ranging data. In Fig. 8 is given the run off of predicted UT1, provided by the U. S. Naval Observatory, from the actual UT1 values, provided by the Bureau International de l'Heure (BIH). In both cases, most of the time, the prediction error is within 5 meters after 10 days. Investigation of the best methods of predicting these phenomena is just beginning. At this stage, these provide the theoretical limit to use of Mode 2 or Mode 4 for calibration. This limitation is true for any satellite based calibration system.

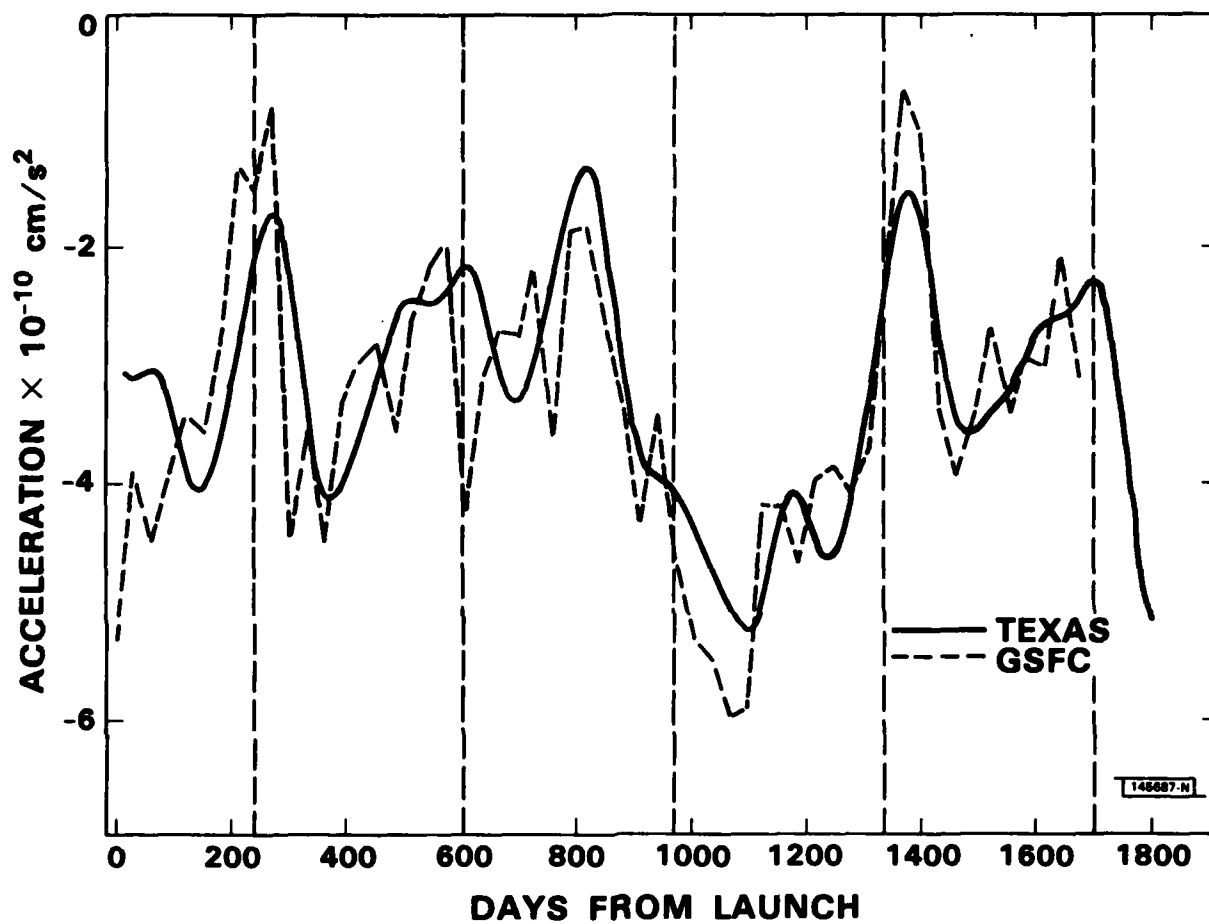


Fig. 7. Days from launch.

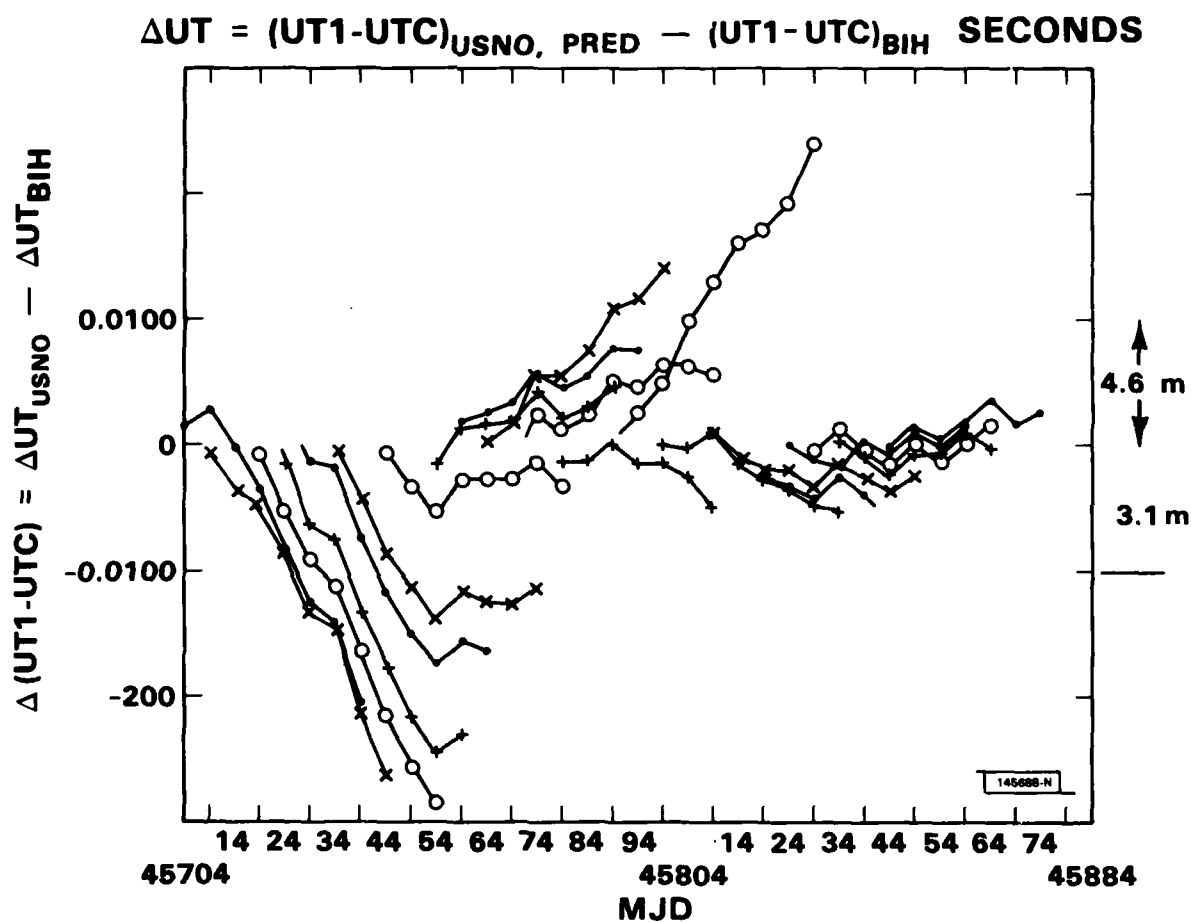


Fig. 8. UT1 prediction.

8. Summary & Conclusions

A method for Radar Calibration has been described and demonstrated. It is apparent that routine 1 m a posteriori calibration is now available when suitable observing procedures are used. It is anticipated that this will be available in real time.

There are three important elements in the observing procedure:

- 1) the tracking mode must be known,
- 2) sufficient number and distribution in elevation of data points must be available, and
- 3) refraction measurements must be made.

A posteriori calibration can be improved, and for the most precise data analysis, these calibration corrections can be applied. All the basic modes of tracking, (coded pulse, frequency domain, time domain) with and without the correlator have different range calibration models. Azimuth and elevation have the same model for each mode. The frequency domain range rate is an unbiased observable with an accuracy of 1 mm/sec . The bias in the time domain range rate has yet to be assessed.

Since September 15, the nominal system calibration has been within $\pm 5\text{ m}$, for the frequency domain tracker. One can speculate that many of the earlier outliers were due to unrecorded system configuration changes. Also, the general

variability of system calibration has decreased with time, and possibly procedures are more faithfully followed. Certainly system calibration variability may be due to a personal equation.

9. Acknowledgements

The initial impetus for this effort came from Dr. R. Sridharan, who also provided the resources. Messrs Kantrowitz and Byers developed the software system for rapid calculation of range bias. Dr. A. Freed computed most of the numerical values. Mr. D. Edge, Bendix Field Services, provided the NASA quick look laser data used in this analysis.

REFERENCES

- (1). R. C. Raup; M. G. Czerwinski, "Best Approximation of Signal Amplitude and Delay in a Narrow-Band Satellite Surveillance System," Technical Report 723, Lincoln Laboratory, M.I.T. (to be published).
- (2). D. Kantrowitz, private communication.
- (3). R. Byers, private communication.
- (4). E. M. Gaposchkin, "The Lorentz Transformation and the Radar Doppler Equation," p. 23, Technical Report 664, Lincoln Laboratory, M.I.T. (15 December 1983) DTIC AD-A137901.
- (5). B. R. Bean, & E. J. Dutton, 1966, Radio Meteorology, NBS Monograph 92, (U. S. Government Printing Office 1 March 1966), p. 435.
- (6). J. A. Klobuchar; M. J. Buonsanto; M. J. Mendillo; & J. M. Johnson, The Contribution of the Plasmasphere to Total Time Delay in Effect of the Ionosphere on Space and Terrestrial Systems, Vol II, Editor J. M. Goodman (U. S. Government Printing Office, 1978), pp. 486-489.
- (7). J. A. Klobuchar & R. S. Allen; "A First-Order Prediction Model of Total-Electron-Content Group Path Delay for Midlatitude Ionosphere," AFCRL 70-0403, Air Force Surveys in Geophysics No. 222, (8 July 1970) p. 20.
- (8). J. Evans; J. M. Holt; W. L. Oliver; R. H. Wand, "The Fossil Theory of Nighttime High Latitude F. Region Troughs," J. Geophys. Res. 88, 7769 (1983).
- (9). F. J. Lerch; S. M. Klosko; & G. B. Patel, "A Refined Gravity Model From Lageos (GEM-L2)," Geophys. Res. Letters 9, 1263 (1982).
- (10). G. H. Kaplan, editor, "The IAU Resolutions of Astronomical Constants, Time Scales and The Fundamental Reference Frame," Naval Observatory Circular No. 163, Washington, DC 20890 (10 Dec 1981), p. 35.
- (11). D. E. Smith; D. C. Christodoulidis; R. Koilenkiewicz; P. J. Dunn; S. M. Klosko; M. H. Torrence; S. Fricke; S. Blackwell; "A Global Geodetic Reference Frame from Lageos Ranging" (SL5.1AP), 1985.

Appendix A

Range Calibration Constants

RANGE CALIBRATION FOR MILLSTONE HILL RADAR FROM LAGEOS ORBIT

MJD	YY	MM	DD	HH	MM	DDD	DR (M)	N	SIGMA (M)	REMARKS	LASER REF
45676.1	83	12	8	3	40	342	19.8	1			
45677.3	83	12	9	9	17	343	9.6	1			
45677.6	83	12	9	16	11	343	16.5	1			
45678.4	83	12	10	11	19	344	14.6	1			
45679.4	83	12	11	10	6	345	14.2	1			
45681.1	83	12	13	3	50	347	17.6	1			
45681.7	83	12	13	17	49	347	-25.7	1		CODED PULSE	
45683.3	83	12	15	8	12	349	9.1	2	2.1		
45684.2	83	12	16	6	57	350	4.2	2	1.0		
45684.7	83	12	16	17	21	350	6.5	2	1.7		
45685.6	83	12	17	15	47	351	16.2	2	0.9		
45686.6	83	12	18			352	17.8	2	0.1		
45687.4	83	12	19			353	6.6	2	2.1		
45688.2	83	12	20			354	11.5	2	0.7		
45688.4	83	12	20			354	9.4	2	1.7		
45690.2	83	12	22			356	13.9	2	0.1		
45692.1	83	12	24			358	18.2	2	1.4		
45692.5	83	12	24			358	13.8	2	0.9		
45694.5	83	12	26			360	16.2	1			
45695.0	83	12	27			361	17.4	1			
45696.1	83	12	28			362	20.7	1			
45698.6	83	12	30			364	17.5	2	0.2		
45699.1	83	12	31			365	15.9	2	0.1		
45700.6	84	1	1			1	13.0	2	0.1		
45701.6	84	1	2			2	7.9	2	0.3		
45702.1	84	1	3			3	9.3	2	0.2		
45703.5	84	1	4			4	4.4	2	0.6		
45704.4	84	1	5			5	-1.8	2	0.3		
45705.6	84	1	6			6	1.1	2	0.2		
45707.4	84	1	8			8	4.4	1			
45710.2	84	1	11			11	11.2	1			
45711.2	84	1	12			12	14.1	1			
45713.1	84	1	14			14	11.3	1			
45713.5	84	1	14			14	17.2	1			
45714.6	84	1	15			15	19.6	2	0.1		
45715.5	84	1	16			16	16.9	2	1.1		
45716.0	84	1	17			17	17.4	2	0.8		
45716.3	84	1	17			17	16.0	2	0.1		
45719.6	84	1	20			20	17.23	1			
45720.4	84	1	21			21	14.70	1			
45723.1	84	1	24			24	9.9	1			
45725.4	84	1	26			26	9.8	2	1.0		
45730.1	84	1	31			31	0.1	2	0.7		

45731.1	84	2	1	32	13.0	2	1.4	
45732.0	84	2	2	33	9.5	2	3.2	
45733.1	84	2	3	34	6.9	1		TIME DOMAIN TRACKER
45733.4	84	2	3	34	6.3	1		TIME DOMAIN TRACKER
45734.0	84	2	4	35	9.3	1		
45735.6	84	2	5	36	9.4	1		
45737.0	84	2	7	38	3.4	1		
45739.3	84	2	9	40	7.9	1		
45740.0	84	2	10	41	14.0	1		
45740.4	84	2	10	41	29.8	1		
45741.1	84	2	11	42	14.6	1		
45744.3	84	2	14	45	9.6	2	3.5	
45744.5	84	2	14	45	18.4	1		
45745.2	84	2	15	46	8.5	1		
45746.1	84	2	16	47	7.8	1		
45747.3	84	2	17	48	12.4	1		
45749.1	84	2	19	50	9.1	2	0.2	
45750.0	84	2	20	51	4.3	2	0.1	
45751.1	84	2	21	52	11.1	2	0.3	
45753.1	84	2	23	54	9.5	1		
45754.1	84	2	24	55	33.3	1		CODED PULSE
45755.3	84	2	25	56	11.4	1		
45756.4	84	2	26	57	18.2	2	0.4	
45758.0	84	2	28	59	16.9	2	1.4	
45760.0	84	3	1	61	18.7	1		
45761.6	84	3	2	62	14.6	1		
45762.3	84	3	3	63	12.7	1		
45765.0	84	3	6	66	13.7	1		
45769.4	84	3	10	70	26.1	2	0.2	
45770.5	84	3	11	71	36.9	2	0.2	
45772.2	84	3	13	73	7.2	2	1.6	
45774.0	84	3	15	75	31.2	2	0.2	
45778.0	84	3	19	79	11.0	2	0.7	
45779.0	84	3	20	80	14.3	2	0.01	
45781.0	84	3	22	82	19.2	1		
45782.9	84	3	23	83	13.4	2	0.9	
45783.3	84	3	24	84	11.9	2	1.0	
45784.4	84	3	25	85	12.8	2	0.9	
45786.4	84	3	27	87	14.5	1		LASER
45787.4	84	3	28	88	31.6	2	2.0	ORBIT
45787.9	84	3	28	88	12.0	2	0.0	31.5
45788.3	84	3	29	89	9.7	2	0.9	10.3
45792.4	84	4	2	93	-17.1	2	0.3	11.0
45793.3	84	4	3	94	-12.7	2	0.7	CODED PULSE -21.1
45795.4	84	4	5	96	13.5	4	0.3	CODED PULSE -19.4
45796.3	84	4	6	97	28.4	4	0.5	14.5
45797.1	84	4	7	98	0.5	3	2.0	30.0
45797.4	84	4	7	98	15.7	3	0.4	2.9
								16.5

45799.0	84	4	9	100	13.6	2	0.4
45800.1	84	4	10	101	9.2	1	
45802.4	84	4	12	103	14.8	1	
45804.5	84	4	14	105	12.9	2	0.3
45805.4	84	4	15	106	14.9	2	0.1
45807.0	84	4	17	108	13.4	2	1.1

RANGE CALIBRATION CONSTANT CHANGED BY +15.0 M

45809.3	84	4	19	110	-2.9	1		
45811.4	84	4	21	112	-1.2	2	0.4	
45813.7	84	4	23	114	3.9	2	3.3	MAX. ELEV. 5°
45813.9	84	4	23	114	6.2	2	0.7	
45814.1	84	4	24	115	-1.7	2	2.0	
45814.3	84	4	24	115	-0.6	2	0.4	
45815.9	84	4	25	116	1.7	1		
45816.4	84	4	26	117	-1.3	1		
45819.9	84	4	29	120	-1.7	2	0.6	
45820.9	84	4	30	121	-11.6	2	0.3	
45821.4	84	5	1	122	-5.2	2	0.7	
45821.7	84	5	1	122	0.5	2	0.5	
45822.3	84	5	2	123	-5.0	2	0.1	
45823.0	84	5	3	124	-2.6	2	0.1	
45824.3	84	5	4	125	-2.1	1		
45825.0	84	5	5	126	-3.5	2	2.7	
45826.4	84	5	6	127	-1.2	2	0.7	
45827.3	84	5	7	128	-2.3	2	0.3	
45827.8	84	5	7	128	-4.9	2	1.1	
45828.3	84	5	8	129	-8.4	2	0.3	
45830.3	84	5	10	131	-36.4	1		NEW TRANS. DRIVER!
45830.8	84	5	10	131	-10.5	1		"
45831.2	84	5	11	132	-39.0	1		"
45832.3	84	5	12	133	-38.8	2	0.9	"
45835.3	84	5	15	136	-39.6	2	3.0	"

RANGE CALIBRATION CONSTANT CHANGED BY -30.0 M

45836.3	84	5	16	137	-7.2	1		CNG RANGE CALIB.
45837.3	84	5	17	138	-6.7	1		
45838.3	84	5	18	139	-5.6	1		
45839.4	84	5	19	140	-8.2	1		
45840.8	84	5	20	141	-5.3	1		
45841.9	84	5	21	142	-7.3	2	0.3	
45842.3	84	5	22	143	-4.1	2	1.8	
45844.0	84	5	24	145	-9.2	1		
45845.3	84	5	25	146	0.9	1		

45846.0	84	5	26	147	-8.9	1		
45847.4	84	5	27	148	2.8	1		
45849.2	84	5	29	150	-2.2	1		
45851.3	84	5	31	152	-3.6	1		
45852.2	84	6	1	153	-9.4	1		
45852.9	84	6	1	153	-3.2	2	1.7	
45853.3	84	6	2	154	-12.2	1		LASER
45854.9	84	6	3	155	-6.1	1		ORBIT
45855.9	84	6	4	156	-7.3	1		-4.6
45857.9	84	6	6	158	-9.8	1		-7.3
45859.3	84	6	8	160	-12.9	1		-9.9
45861.3	84	6	10	162	-10.3	1		-13.5
45863.3	84	6	12	164	-10.1	1		-10.5
45864.8	84	6	13	165	-7.8	1		-8.9
45865.2	84	6	14	166	-7.8	1		-8.6
45866.3	84	6	15	167	3.6	1		-9.8
45867.0	84	6	16	168	-11.6	1		3.7
45868.4	84	6	17	169	-7.3	1		-8.9
45870.3	84	6	19	171	3.3	2	3.3	-7.8
45872.3	84	6	21	173	-12.6	1		-3.7
45873.2	84	6	22	174	-5.8	1		-13.2
45874.3	84	6	23	175	-1.5	1		-4.9
45875.8	84	6	24	176	5.2	1		
45876.3	84	6	25	177	-3.9	2	1.5	
45878.9	84	6	27	179	-9.8	2	0.0	
45883.9	84	7	2	184	-11.0	2	0.2	
45884.8	84	7	3	185	-7.1	2	0.0	
45886.2	84	7	5	187	-6.5	3	0.9	
45887.3	84	7	6	188	-3.2	3	2.3	
45889.8	84	7	8	190	-4.5	3	0.7	
45890.0	84	7	9	191	-9.1	3	1.5	
45891.2	84	7	10	192	-4.8	5	2.8	
45894.2	84	7	13	195	-6.7	4	0.6	
45895.3	84	7	14	196	-4.7	4	0.9	
45896.2	84	7	15	197	-7.2	4	0.4	
45896.7	84	7	15	197	-6.6	4	0.7	
45898.1	84	7	17	199	-11.6	3	1.1	
45900.1	84	7	19	201	-7.4	3	0.9	
45901.2	84	7	20	202	-5.4	3	0.9	
45901.9	84	7	20	202	-9.7	2	0.1	
45905.7	84	7	24	206	-8.4	3	0.6	
45906.2	84	7	25	207	11.9	3	0.5	
45906.8	84	7	25	207	14.2	2	0.3	
45908.3	84	7	27	209	12.6	4	0.5	
45908.8	84	7	27	209	19.1	4	1.3	
45910.7	84	7	29	211	14.7	4	2.1	
45912.0	84	7	31	213	8.0	5	0.6	
45912.9	84	7	31	213	10.8	4	1.2	

45913.1	84	8	1	214	11.2	4	0.5
45913.9	84	8	1	214	4.4	3	0.2
45915.2	84	8	3	216	21.7	3	0.3
45915.7	84	8	3	216	19.8	3	0.2
45917.7	84	8	5	218	21.3	3	0.4
45919.1	84	8	7	220	-5.6	2	0.2
45922.7	84	8	10	223	-6.1	1	
45924.8	84	8	12	225	-3.6	2	0.4
45926.6	84	8	14	227	11.1	2	1.0
45927.1	84	8	15	228	-8.4	2	0.2
45927.9	84	8	15	228	-12.2	2	1.9
45929.1	84	8	17	230	-6.7	2	2.5
45929.1	84	8	17	230	-6.7	2	2.5
45929.8	84	8	17	230	-6.8	2	0.6
45932.7	84	8	19	232	-1.3	3	0.9
45933.2	84	8	21	234	2.4	2	0.3
45933.7	84	8	21	234	-3.7	2	0.0
45935.2	84	8	23	236	-5.2	2	0.7
45936.2	84	8	24	237	-1.1	3	0.5
45936.7	84	8	24	237	-6.1	3	0.8
45936.8	84	8	24	237	-7.3	3	1.8
45938.7	84	8	26	239	-3.7	3	0.3
45940.1	84	8	28	241	-5.1	3	1.5
45941.2	84	8	29	242	-3.0	3	0.5
45943.7	84	8	31	244	-6.2	3	0.8
45944.0	84	9	1	245	-8.1	4	2.1
45944.1	84	9	1	245	-6.1	4	0.4
45947.0	84	9	4	248	-3.3	2	1.3
45950.8	84	9	7	251	-5.0	2	0.7
45951.7	84	9	8	252	-3.9	2	0.5
45954.8	84	9	11	255	-6.6	2	1.1
45955.0	84	9	12	256	-6.1	2	0.2
45957.6	84	9	14	258	-4.3	1	
45958.7	84	9	15	259	1.3	1	
45959.0	84	9	16	260	0.3	1	
45961.0	84	9	18	262	0.2	2	0.2
45962.9	84	9	19	263	2.6	2	0.9
45964.2	84	9	21	265	7.2	2	1.3
45968.6	84	9	25	269	1.1	1	
45972.7	84	9	29	273	-5.8	4	1.0
45973.6	84	9	30	274	-0.9	4	0.6
45975.1	84	10	2	276	3.9	4	1.3
45975.7	84	10	2	276	3.8	4	0.3
45977.0	84	10	4	278	-1.2	5	0.4
45979.1	84	10	6	280	18.0	5	0.6
45980.7	84	10	7	281	-0.4	4	1.3
45981.6	84	10	8	282	-1.7	4	1.4
45981.9	84	10	8	282	-4.0	4	3.8

TIME DOMAIN TRACK

45983.0	84	10	10	284	-1.3	3	0.9	
45983.1	84	10	10	284	0.6	3	1.4	
45983.9	84	10	10	284	-7.6	2	1.7	
45984.1	84	10	11	285	1.2	3	0.7	
45985.0	84	10	12	286	-1.3	2	0.1	
45986.8	84	10	13	287	-0.3	2	1.6	
45987.9	84	10	14	288	2.5	2	1.2	
45988.9	84	10	15	289	0.0	2	0.0	
45989.1	84	10	16	290	-1.5	2	0.6	
45993.9	84	10	20	294	0.3	2	0.2	
45996.8	84	10	23	297	3.3	2	0.9	
45998.0	84	10	25	299	2.0	2	0.2	
45999.6	84	10	26	300	1.9	3	0.1	
46000.0	84	10	27	301	2.4	3	0.6	
46000.6	84	10	27	301	4.0	3	0.8	
46003.0	84	10	30	304	1.5	3	0.2	
46005.1	84	11	1	306	2.5	3	1.0	
46006.7	84	11	2	307	2.2	2	1.1	
46006.8	84	11	2	307	-2.3	2	1.3	
46008.5	84	11	4	309	9.5	1		CORRELATOR
46009.0	84	11	5	310	-0.3	4	0.8	
46012.0	84	11	8	313	0.4	3	1.2	
46013.6	84	11	9	314	-2.1	2	0.3	
46014.0	84	11	10	315	-5.9	2	0.4	
46014.6	84	11	10	315	14.0	2	0.0	CORRELATOR
46017.0	84	11	13	318	-0.5	3	1.2	
46018.0	84	11	14	319	-0.8	2	0.3	
46019.0	84	11	15	320	1.0	3	0.3	
46020.6	84	11	16	321	-0.6	2	0.9	
46021.0	84	11	17	322	1.8	2	0.1	
46022.9	84	11	18	323	-35.5	2	1.1	CODED PULSE
46027.6	84	11	23	328	7.0	3	1.4	
46027.8	84	11	23	328	-5.5	3	2.8	ONLY 15 OBSER
46027.9	84	11	23	328	-1.0	3	2.1	
46028.6	84	11	24	329	15.2	3	0.1	CORRELATOR
46029.5	84	11	25	330	16.8	3	1.4	CORRELATOR
46031.6	84	11	27	332	-2.3	3	0.3	
46032.9	84	11	28	333	-2.2	3	0.9	
46034.5	84	11	30	335	0.2	4	0.3	
46034.7	84	11	30	335	-6.7	4	0.4	
46034.8	84	11	30	335	-26.8	1		ONLY 8 CODED OBSER
46035.0	84	12	1	336	-1.8	4	0.4	
46035.5	84	12	1	336	-1.8	4	0.3	
46036.6	84	12	2	337	-2.8	4	0.4	
46038.4	84	12	4	339	-3.6	3	0.1	
46040.0	84	12	6	341	-3.6	3	0.9	
46041.6	84	12	7	342	-4.3	2	0.5	
46041.9	84	12	7	342	-6.5	2	0.8	

46042.5	84	12	8	343	-3.1	4	0.4
46043.5	84	12	9	344	-3.1	4	0.1
46045.0	84	12	11	346	-5.7	3	0.3
46045.5	84	12	11	346	-4.2	3	0.2
46046.9	84	12	12	347	-3.4	3	0.4
46047.0	84	12	13	348	-3.6	3	0.5
46048.0	84	12	14	349	5.0	2	0.4
46048.5	84	12	14	349	2.2	2	0.1
46049.6	84	12	15	350	-1.6	2	0.3
46050.5	84	12	16	351	0.2	2	0.1
46051.4	84	12	17	352	1.5	2	0.1
46051.9	84	12	17	352	-0.8	2	0.4

UNCLASSIFIED

SECURITY CLASSIFICATION OF THIS PAGE (When Data Entered)

REPORT DOCUMENTATION PAGE		READ INSTRUCTIONS BEFORE COMPLETING FORM
1. REPORT NUMBER ESD-TR-85-173	2. GOVT ACCESSION NO. AD-A160 362	3. RECIPIENT'S CATALOG NUMBER
4. TITLE (and Subtitle) Metric Calibration of the Millstone Hill L-Band Radar		5. TYPE OF REPORT & PERIOD COVERED Technical Report
		6. PERFORMING ORG. REPORT NUMBER Technical Report 721
7. AUTHOR(s) Edward M. Gaposchkin		8. CONTRACT OR GRANT NUMBER(s) F19628-85-C-0002
9. PERFORMING ORGANIZATION NAME AND ADDRESS Lincoln Laboratory, M.I.T. P.O. Box 73 Lexington, MA 02173-0073		10. PROGRAM ELEMENT, PROJECT, TASK AREA & WORK UNIT NUMBERS Program Element Nos. 63428F and 12424F Project Nos. 2698 and 2295
11. CONTROLLING OFFICE NAME AND ADDRESS Air Force Systems Command, USAF Andrews AFB Washington, DC 20334		12. REPORT DATE 19 August 1985
		13. NUMBER OF PAGES 70
14. MONITORING AGENCY NAME & ADDRESS (if different from Controlling Office) Electronic Systems Division Hanscom AFB, MA 01731		15. SECURITY CLASS. (of this Report) Unclassified
		16a. DECLASSIFICATION DOWNGRADING SCHEDULE
18. DISTRIBUTION STATEMENT (of this Report) Approved for public release; distribution unlimited.		
17. DISTRIBUTION STATEMENT (of the abstract entered in Block 20, if different from Report)		
18. SUPPLEMENTARY NOTES None		
19. KEY WORDS (Continue on reverse side if necessary and identify by block number) calibration , radar calibration , extended range calibration , laser ranging , Lageos , precision orbit determination , refraction		
20. ABSTRACT (Continue on reverse side if necessary and identify by block number) The precision Lageos orbit is used for near real time calibration of the Millstone Hill Radar 1 MHz chirped frequency domain tracker. With independent tracking data, the range calibration is given to ~ 1 m, with Millstone data the range calibration is given to ~ 5 m. The range rate is an unbiased measurement, with an accuracy of ~ 1 mm/sec. The azimuth and elevation are calibrated to $0^{\circ}.020$ and $0^{\circ}.002$ respectively. Tables of calibration constants are given. 0.020 deg		

DD FORM
1 Jan 73

1473

EDITION OF 1 NOV 65 IS OBSOLETE

UNCLASSIFIED

SECURITY CLASSIFICATION OF THIS PAGE (When Data Entered)

END

FILMED

11-85

DTIC